Overview of Beam Energy Scan Program

Lijuan Ruan (BNL)

June 12, 2024

2024 RHIC/AGS Annual Users' Meeting, Beam Energy Scan Workshop

RHIC @ Brookhaven National Laboratory

24 years of RHIC operation

The mission of RHIC

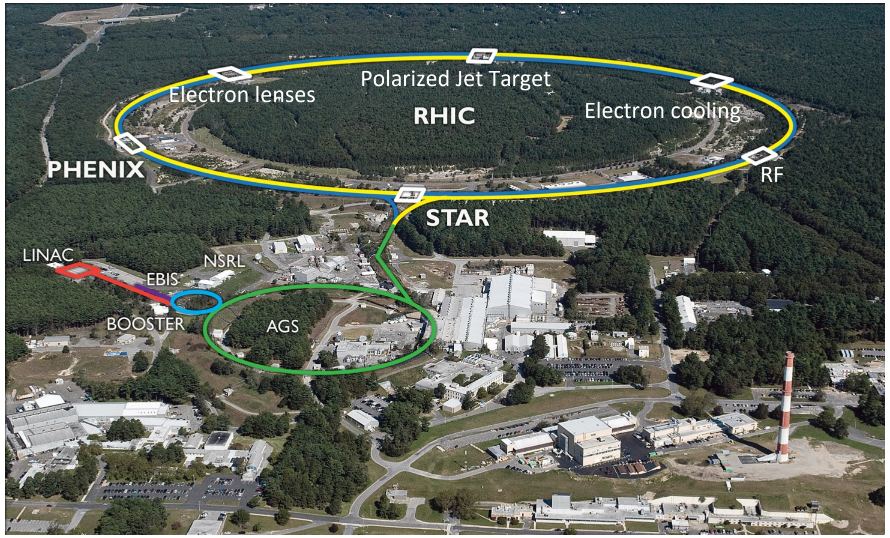

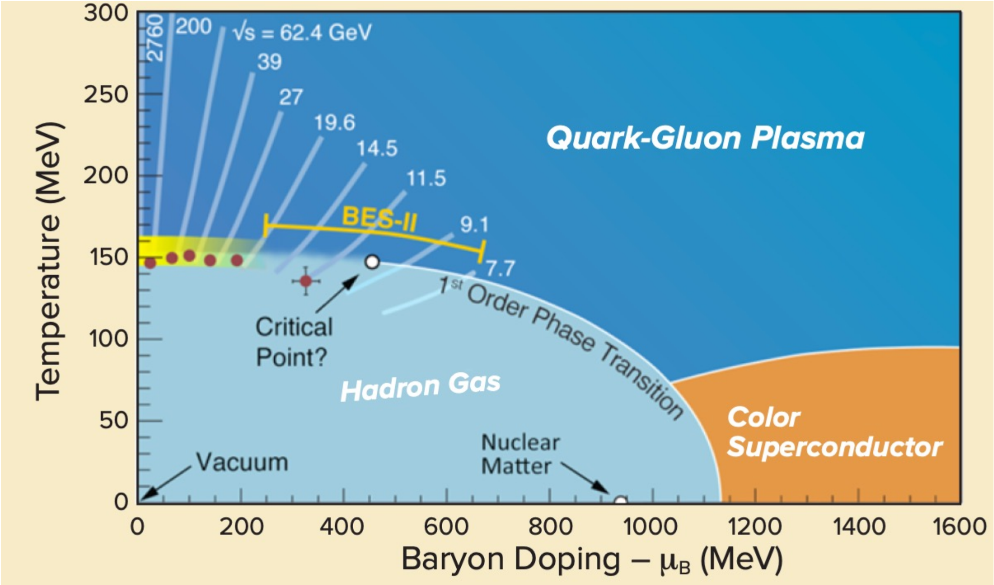

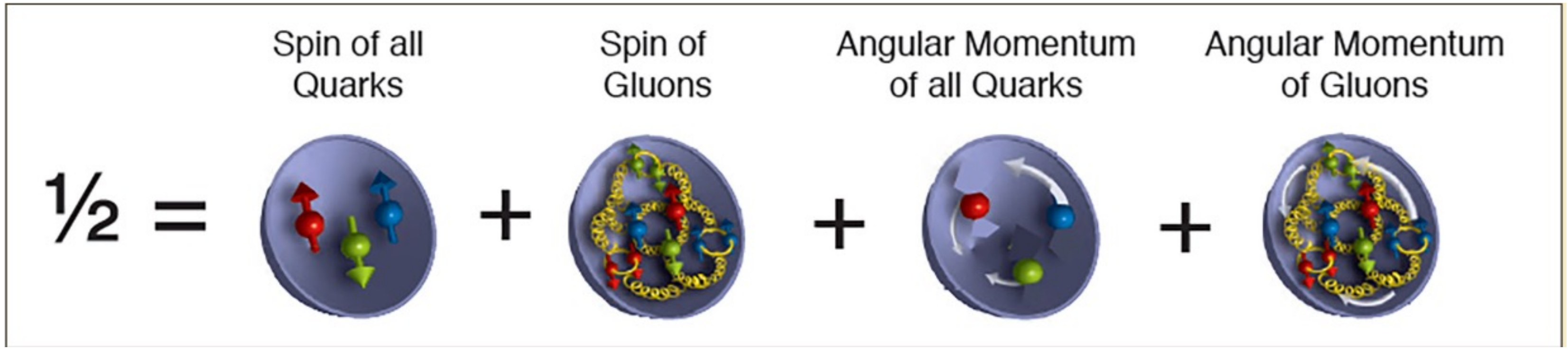

To probe the inner workings of the Quark-Gluon Plasma

To map the phase diagram of QCD

To study the spin puzzle of proton

The phases of QCD matter

Lattice QCD: crossover chiral transition at $\mathbf{\mu_B < 2\,T}$

At top RHIC and LHC energies, measurements consistent with a smooth crossover chiral transition

Change T and $\mathbf{\mu_B}$ by varying the collision energy:

- Search for the critical point
- Search for the first-order phase transition
- Search for the threshold of QGP formation

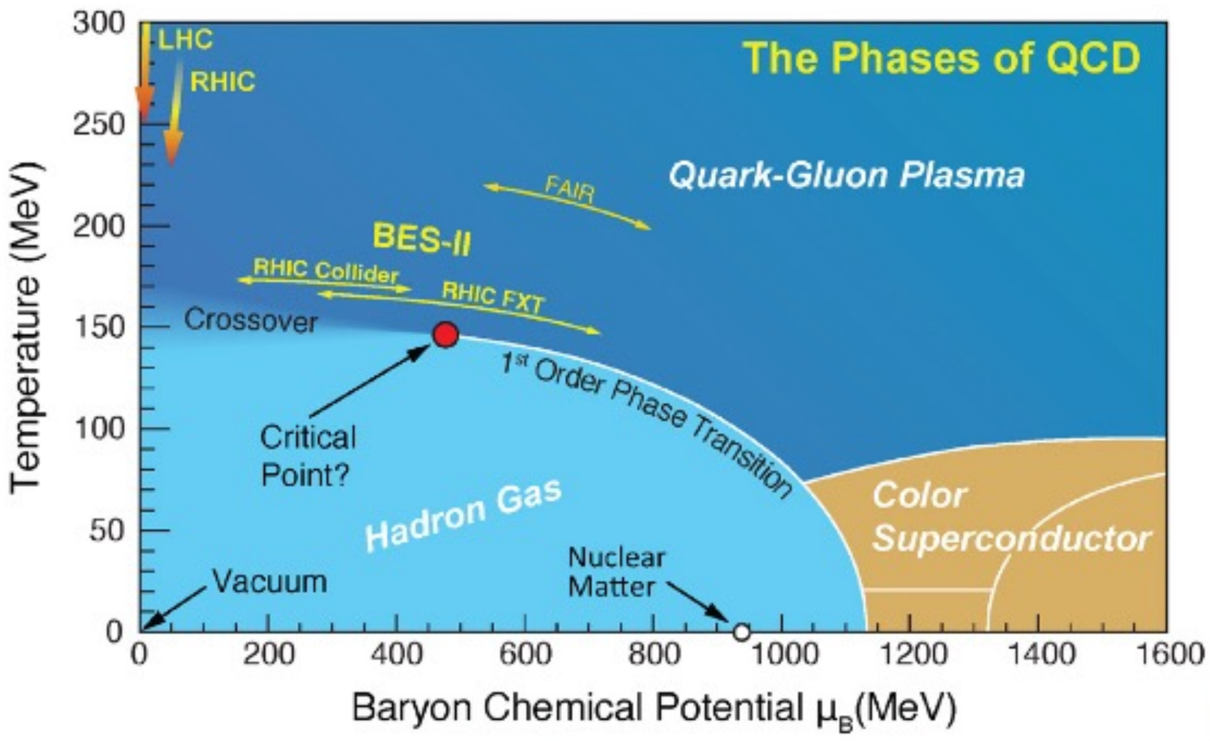

STAR beam energy scan phase I campaign

RHIC Multi-Year Beam Use Request
For Run7 – Run 9

The STAR Collaboration

August 24, 2006

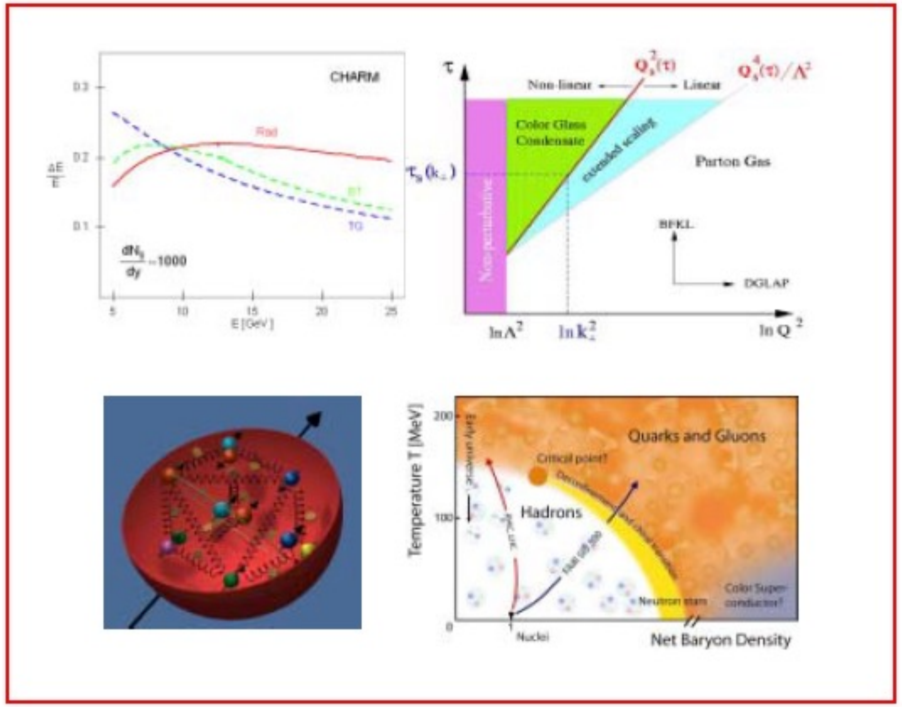

In 2006, stated in the Beam Use Request:
definite search for the existence and location of the QCD Critical Point for Run 2009

RHIC Beam Energy Scan Phase I in 2010 and 2011

Energy (GeV)	7.7	11.5	19.6	27	39	62.4	200
Statistics (Million)	~3	~6.6	~15	~30	~87	~47	~242
Year	2010	2010	2011	2011	2010	2010	2010

Time of flight detector upgrade just completed before Run 2010

The STAR detector in 2010 and 2011

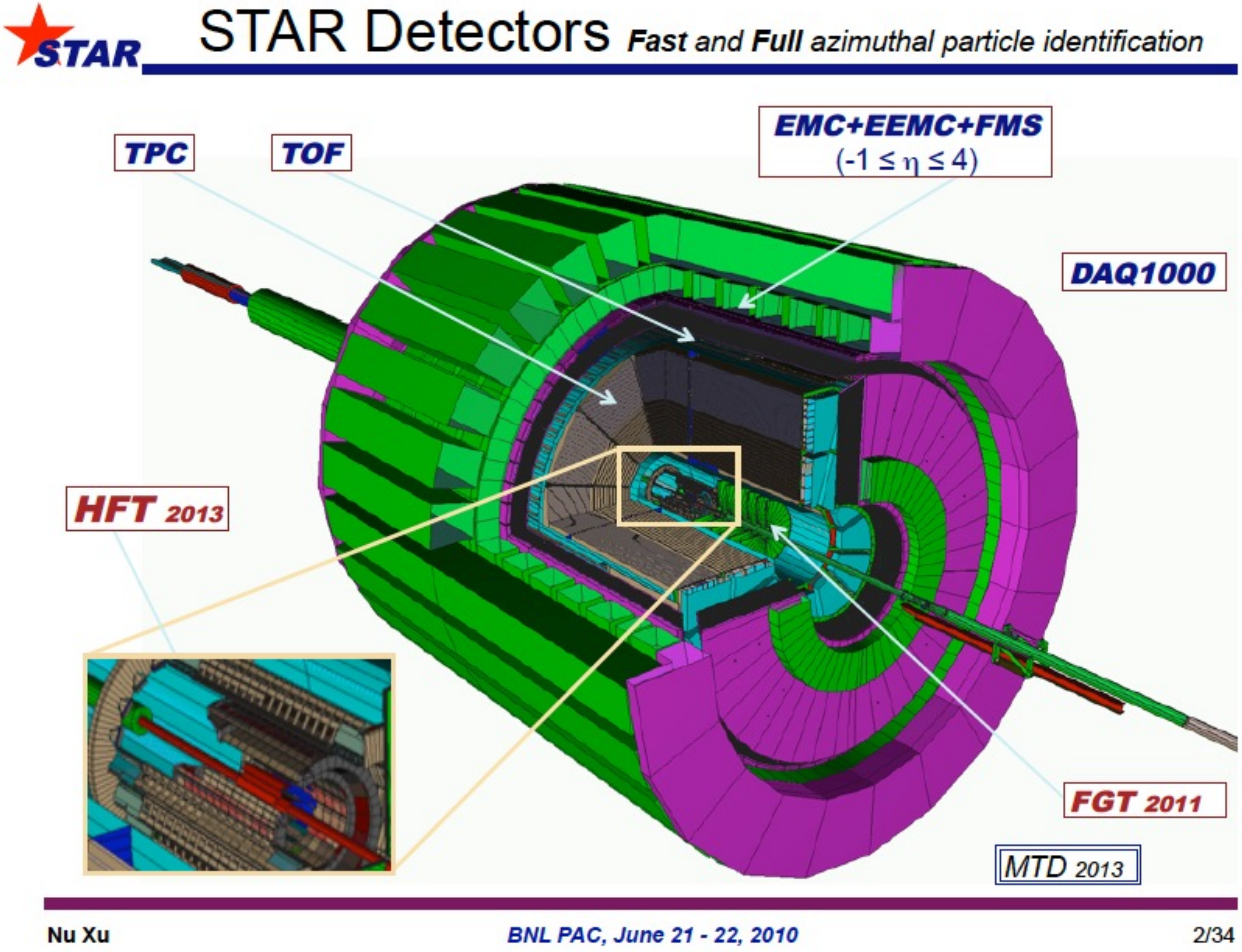

Particle identification with TPC+TOF

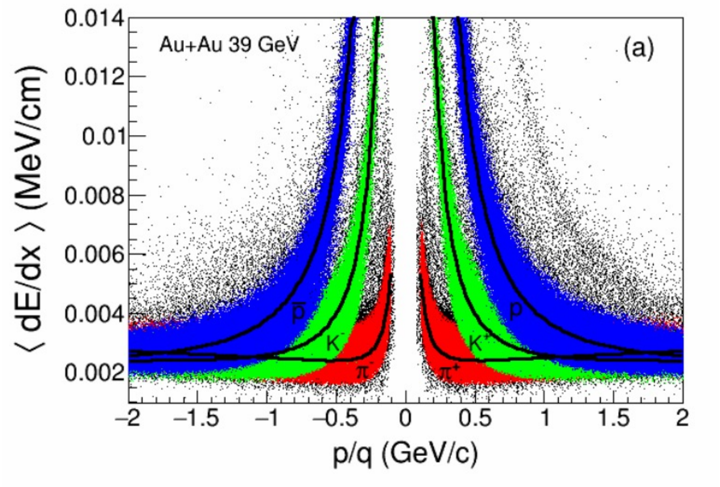

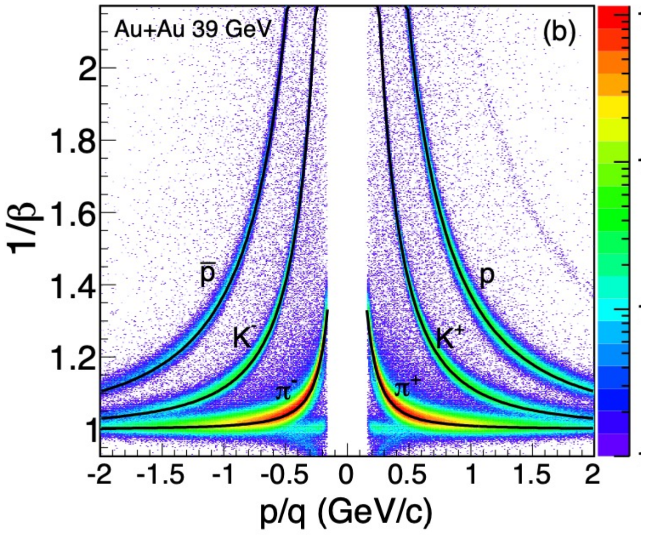

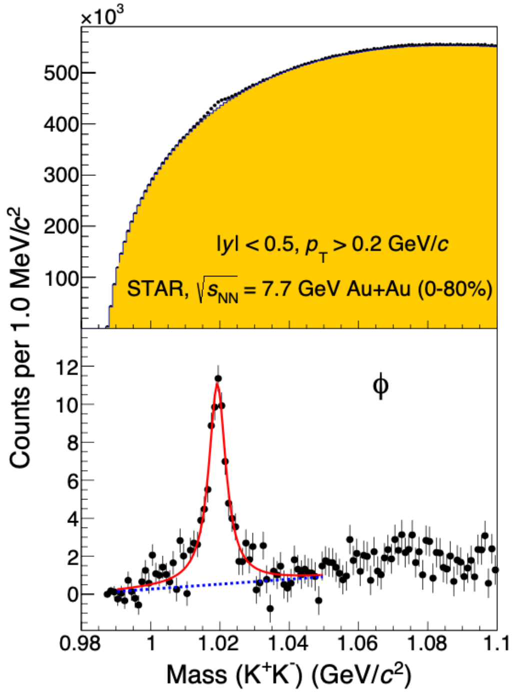

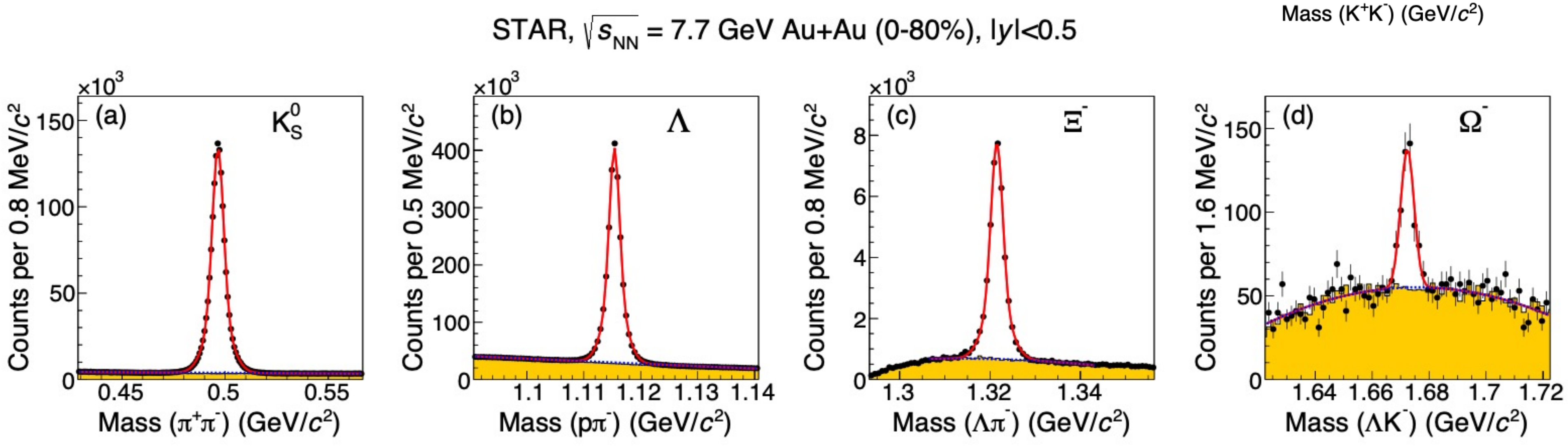

Measure T and μ_B

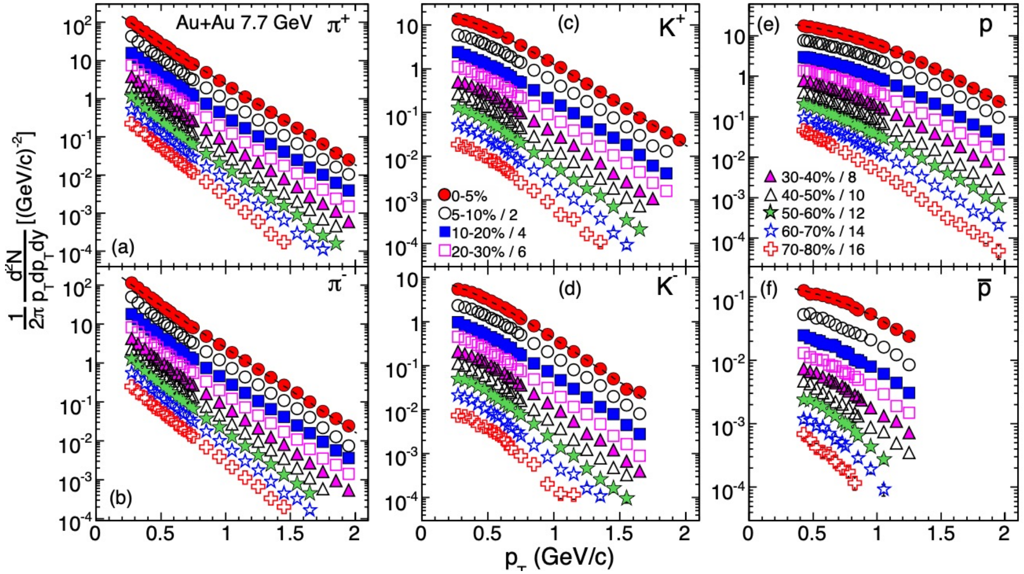

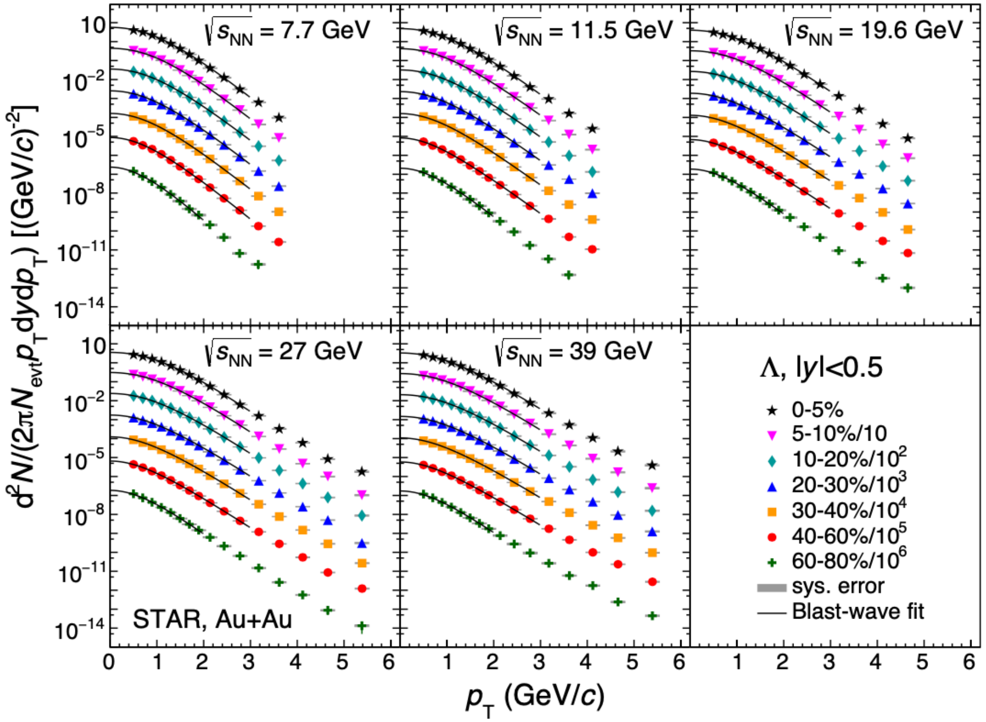

Phys. Rev. C 96 (2017) 44904

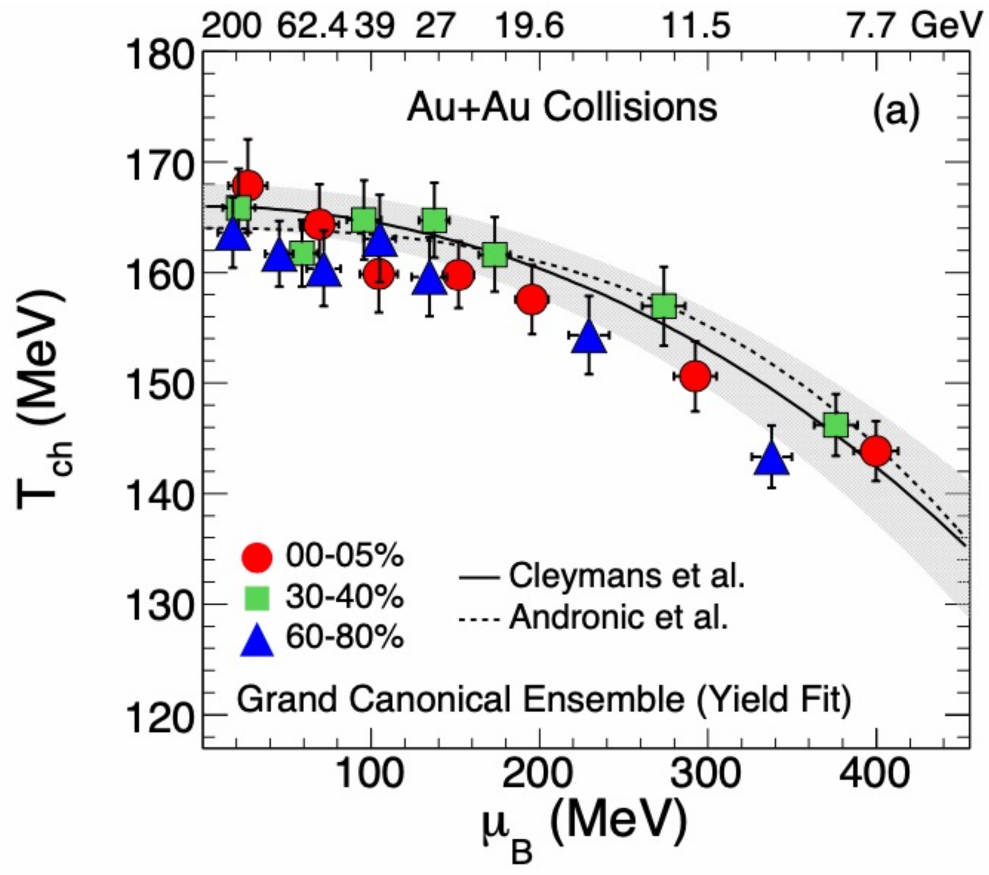

$\pi^{\pm}$, $K^{\pm}$, p, $\bar{p}$, Λ, $\bar{\Lambda}$, Ξ, and $\overline{\Xi}$.

π^-/π^+, K^-/K^+, $\bar{p}/p$, $\bar{\Lambda}/\Lambda$, $\overline{\Xi}/\Xi$, K^-/π^-, $\bar{p}/\pi^-$, Λ/π^-, and $\overline{\Xi}/\pi^-$.

Photons and dileptons

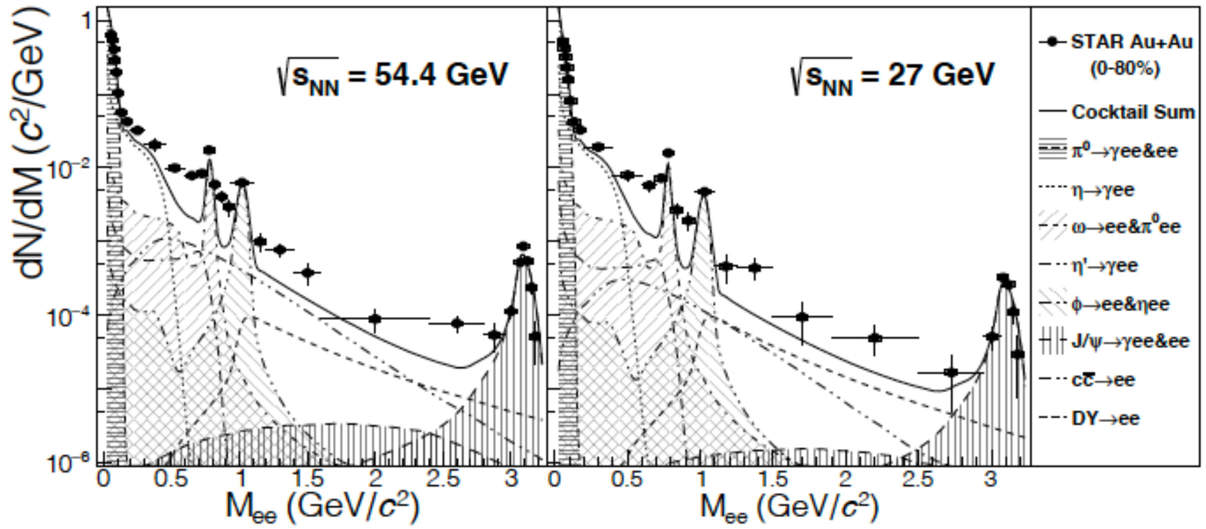

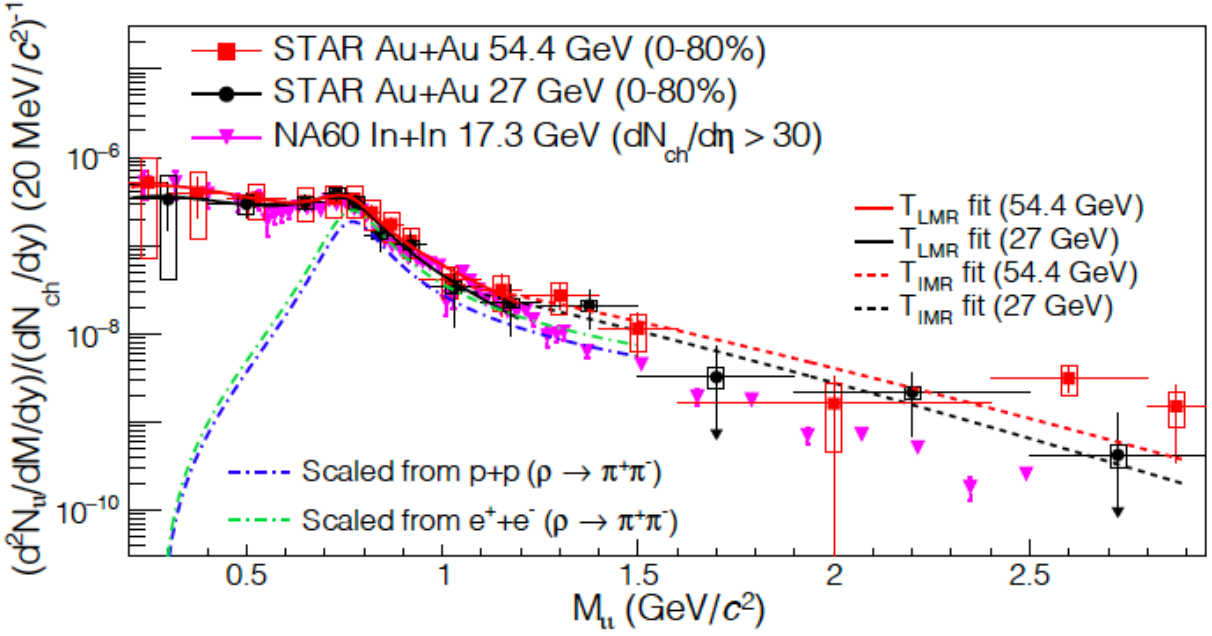

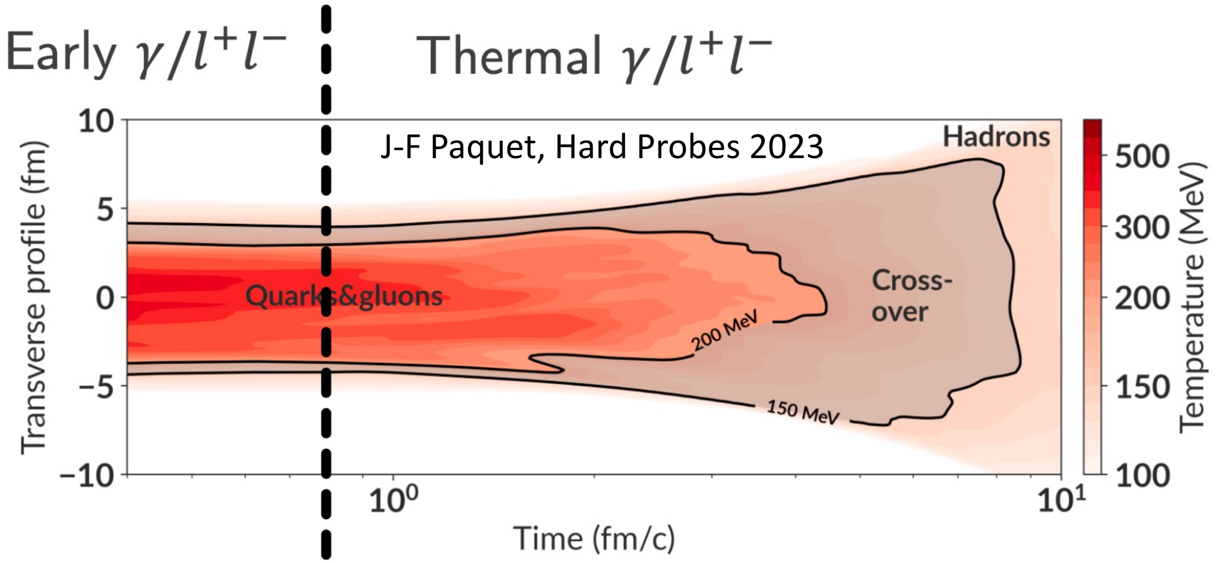

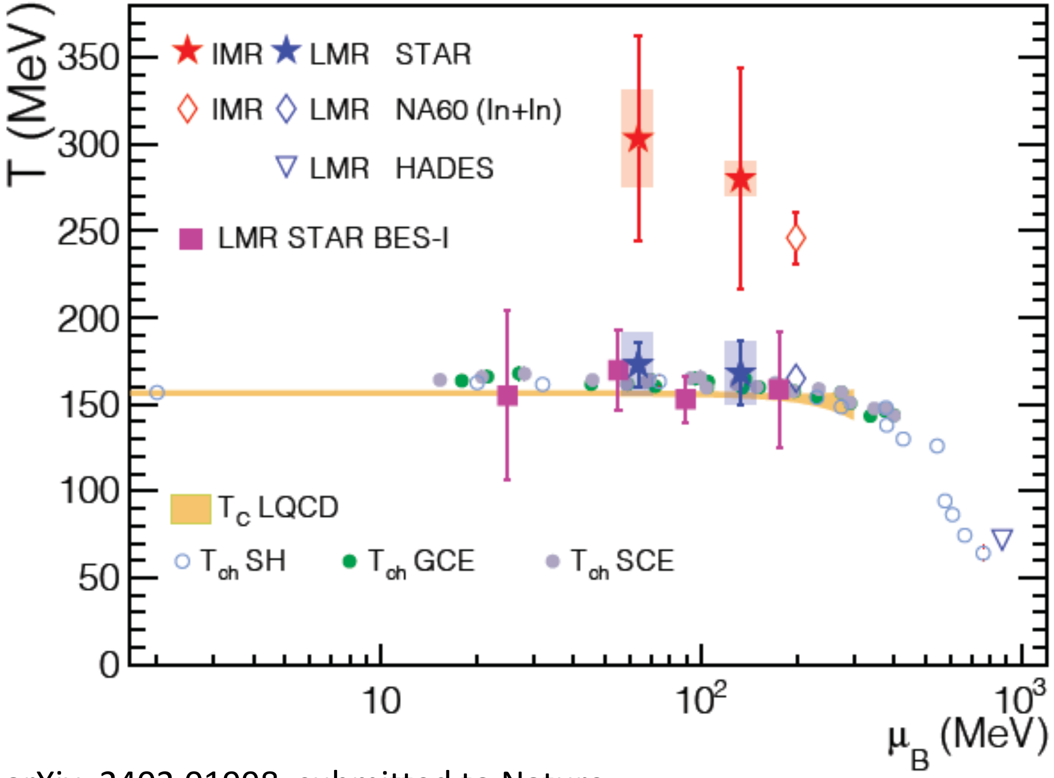

arXiv: 2402.01998, submitted to Nature

How to infer the QCD critical point

Divergence of the correlation length, dynamics slow down, Large density fluctuations

Critical opalescence, magnetic susceptibility

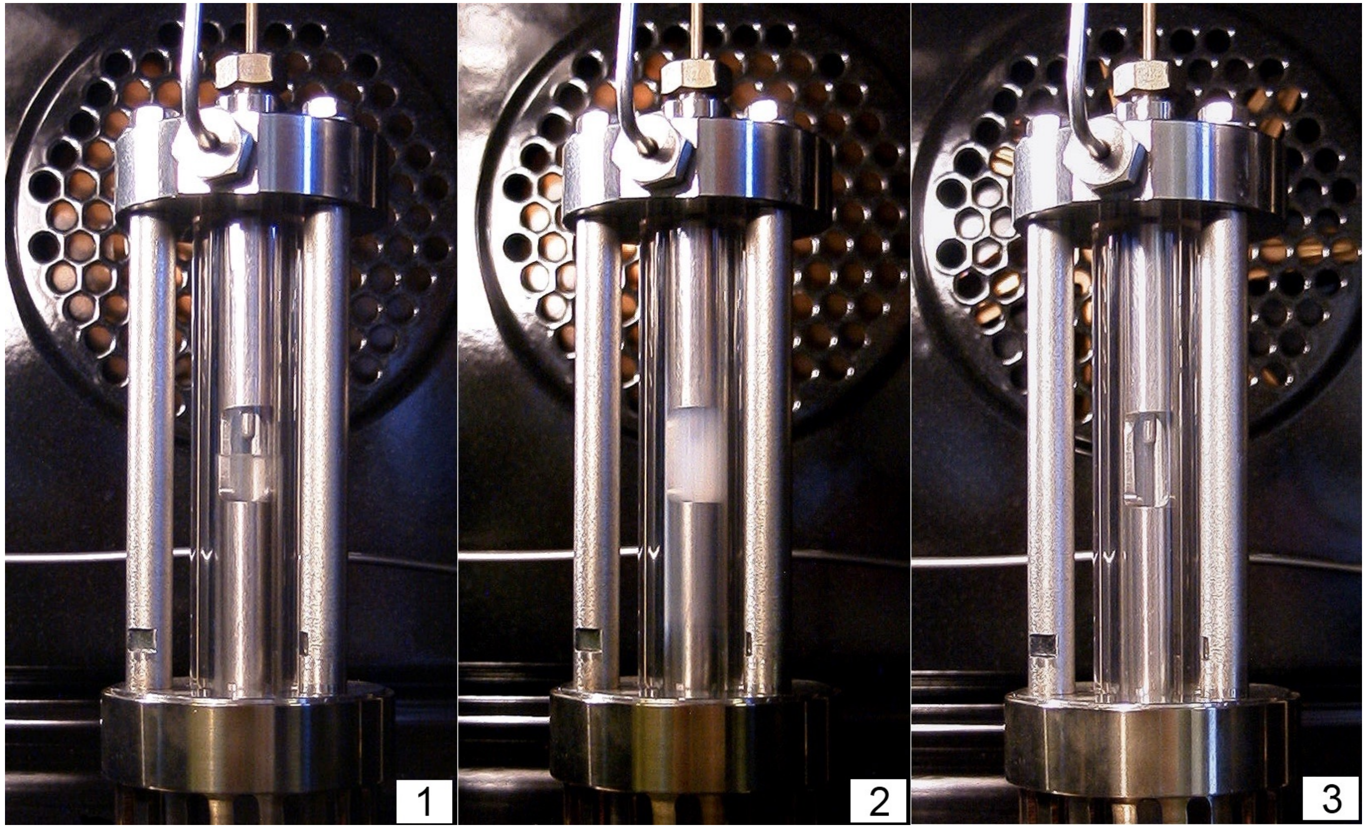

How to infer the QCD critical point

Correlation length related to various moments of the distributions of conserved quantities such as net-baryon, net-charge, and net-strangeness.

$$<(\delta N)^2> \approx \xi^2, <(\delta N)^3> \approx \xi^{4.5}, <(\delta N)^4> -3<(\delta N)^2>^2 \approx \xi^7$$

Mean: $M = <N>$

St. Deviation: $\sigma = \sqrt{<(N-<N>)^2>}$

Skewness: $S = \frac{<(N-<N>)^3>}{\sigma^3}$

Kurtosis: $\kappa = \frac{<(N-<N>)^4>}{\sigma^4} - 3$

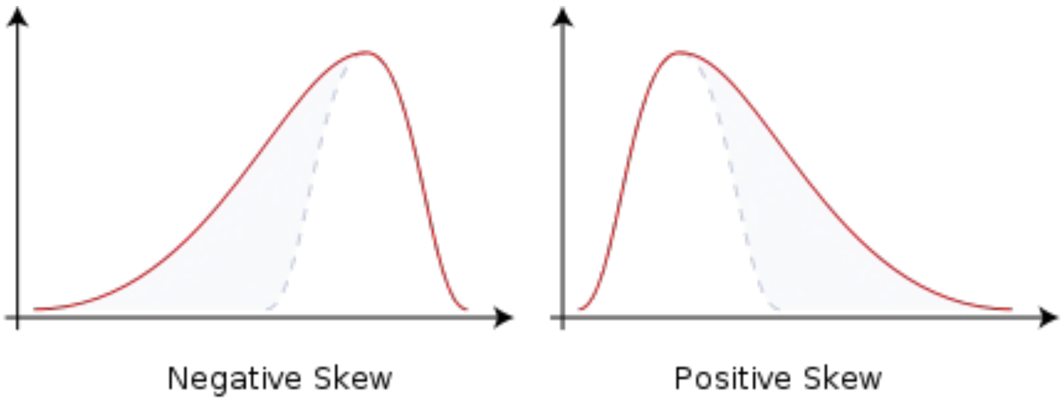

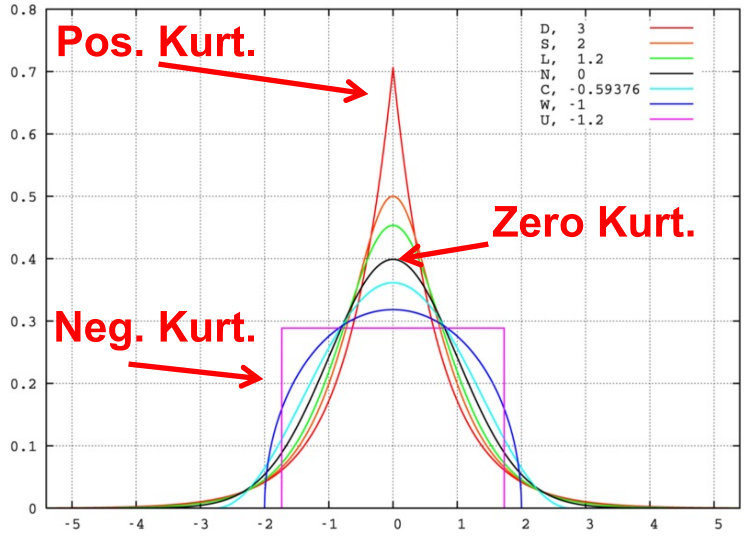

Measure non-Gaussian fluctuation of conserved quantities

Connection to Lattice QCD

Lattice calculations show that moments of the conserved charge (net-baryon, net-charge, net-strangeness) distributions are related to the susceptibilities

Pressure:

$$\frac{p}{T^4} = \frac{1}{VT^3} \ln Z(V, T, \mu_B, \mu_Q, \mu_S)$$

Susceptibility:

$$\chi_q^{(n)} = \frac{1}{T^4} \frac{\partial^n}{\partial(\mu_q / T)^n} P\left(\frac{T}{T_C}, \frac{\mu_q}{T}\right)\Big|_{T/T\,c},$$

$q = B, Q, S$ **(Conserved Quantum Number)**

$$\chi_q^{(1)} = \frac{1}{VT^3}\langle \delta N_q \rangle, \chi_q^{(2)} = \frac{1}{VT^3}\langle (\delta N_q)^2 \rangle$$

$$\chi_q^{(3)} = \frac{1}{VT^3}\langle (\delta N_q)^3 \rangle$$

$$\chi_q^{(4)} = \frac{1}{VT^3}\left(\langle (\delta N_q)^4 \rangle - 3\langle (\delta N_q)^2 \rangle^2\right)$$

A. Bazavov et al *.arXiv::1208.1220. 1207.0784.*
F. Karsch et al, PLB 695, 136 (2011).
arXiv: 1203.0784; S. Borsanyi et al, JHEP1201,138(2011);

Net-proton higher moments from BES-I with TOF

PRL 126 (2021) 92301

20 < μ_B < 420 MeV

pT range extended to 0.4-2 GeV/c

14.5 and 54.4 GeV data included

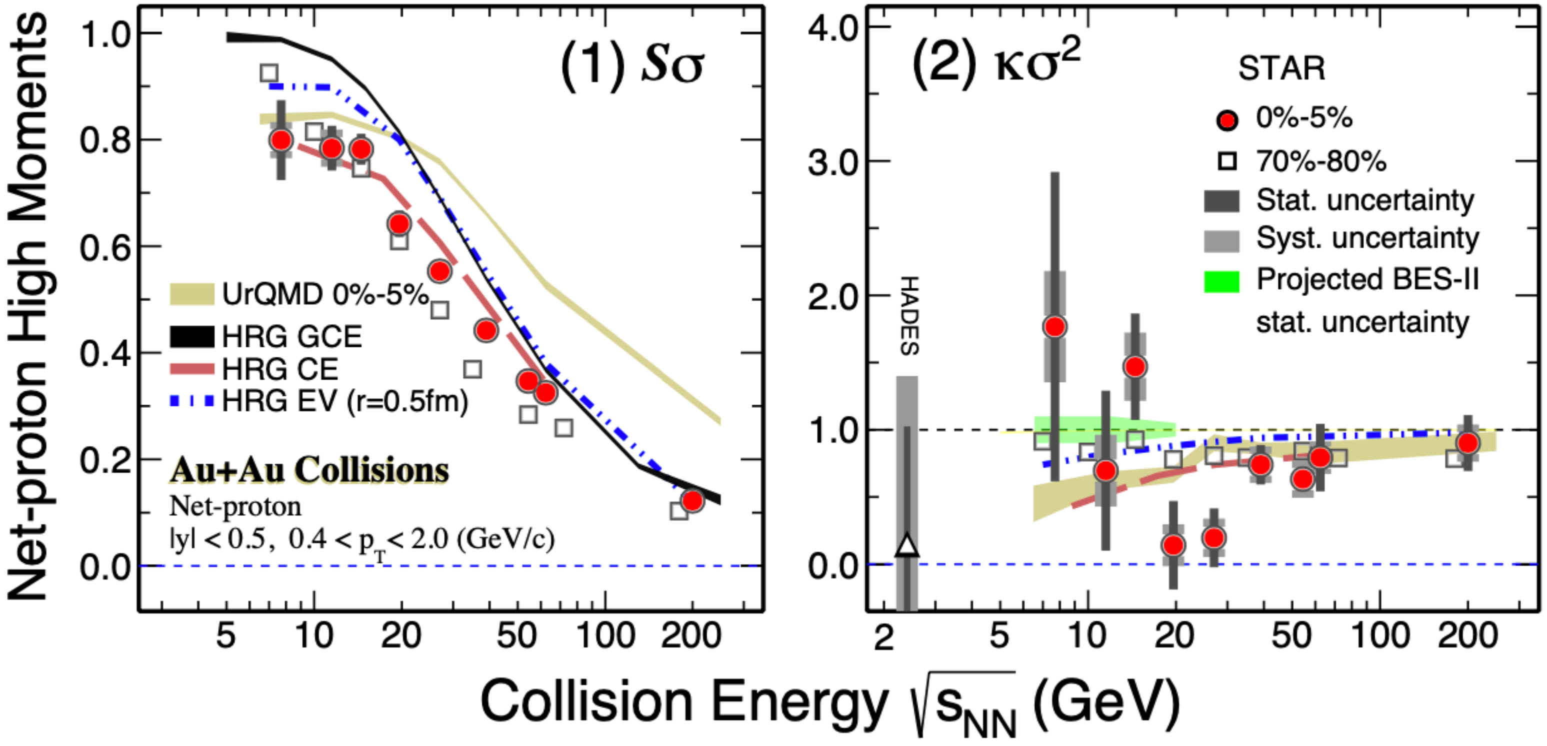

First evidence of a non-monotonic variation in kurtosis times variance of the net-proton number distribution as a function of collision energy with 3.1 sigma significance

Light nuclei yield ratio

PRL 130 (2023) 202301

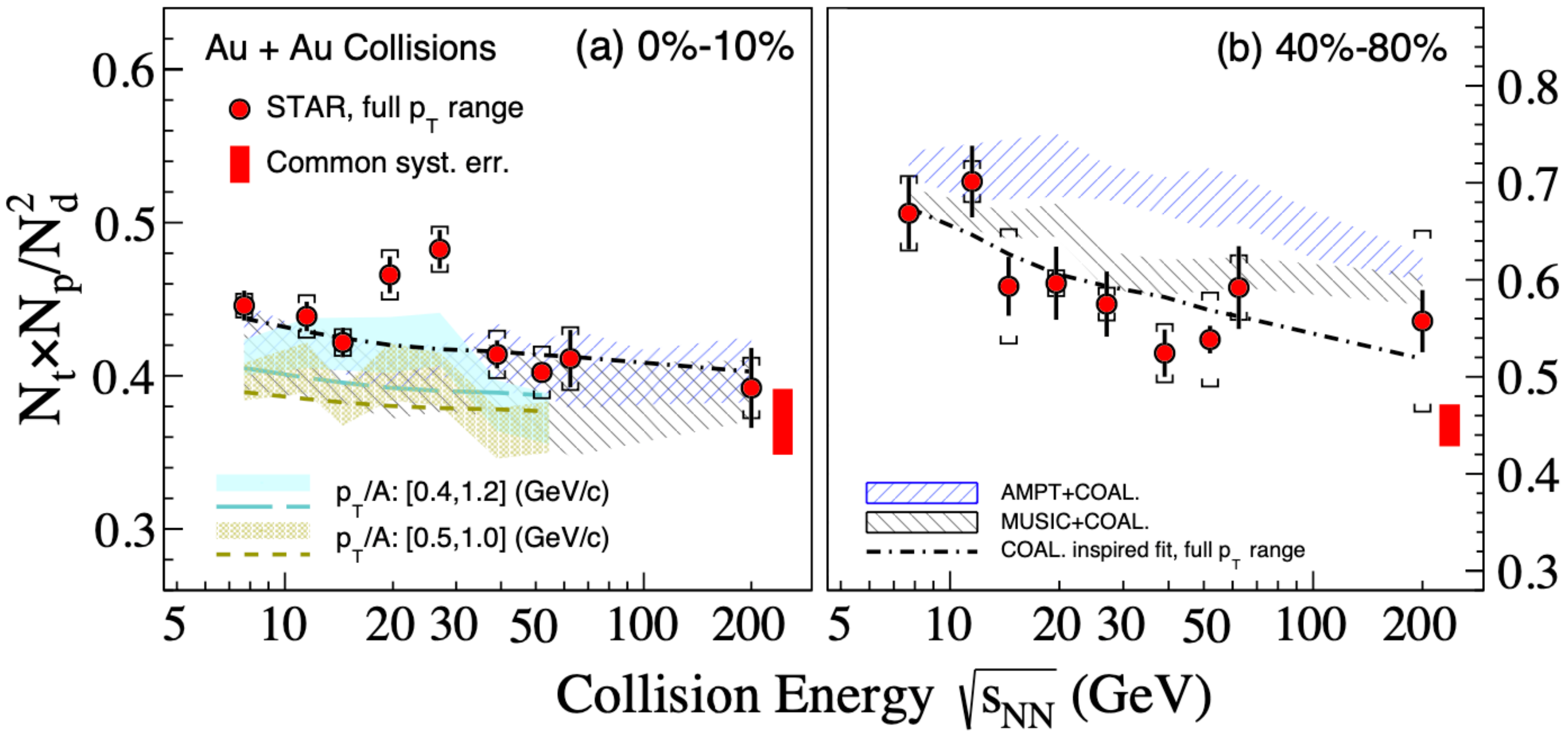

N_tN_p/N_d^2, sensitive to fluctuations of the local neutron density shows enhancements relative to the coalescence baseline with a significance of 2.3σ and 3.4σ respectively in 0 –10% central Au+Au collisions at 19.6 and 27 GeV.

Constrain production dynamics of light nuclei and understanding of the QCD phase diagram

Beam energy dependence of identified particle v_1 slope

Directed flow: first harmonic in the Fourier expansion of the azimuthal distribution of produced particles with respect to the reaction plane

$$\frac{dN}{d(\phi - \Psi_{RP})} = k\{1 + \sum_{n=1}^{\infty} 2v_n \cos[n(\phi - \Psi_{RP})]\}$$

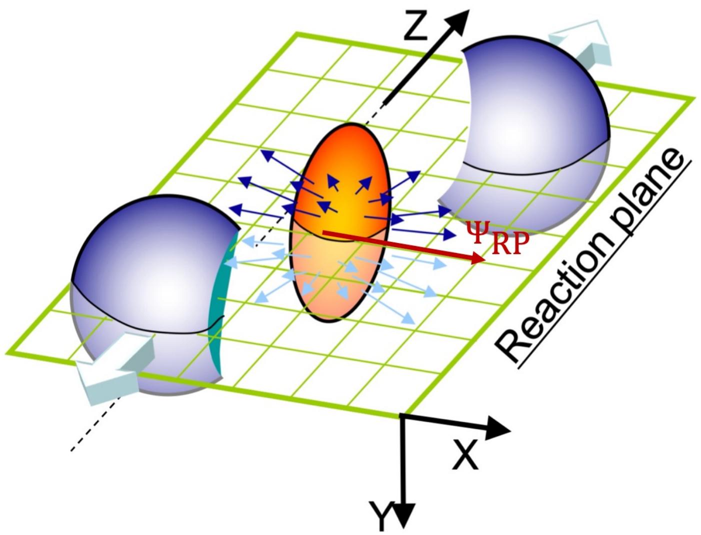

Describes collective sideward motion of produced particles and nuclear fragments and carries information on the very early stages of the collision

A.M. Poskanzer and S.A. Voloshin, Phys. Rev. C 58, 1671(1998)

Phys. Rev. Lett. **120** (2018) 62301
Phys. Rev. Lett. **112** (2014) 162301

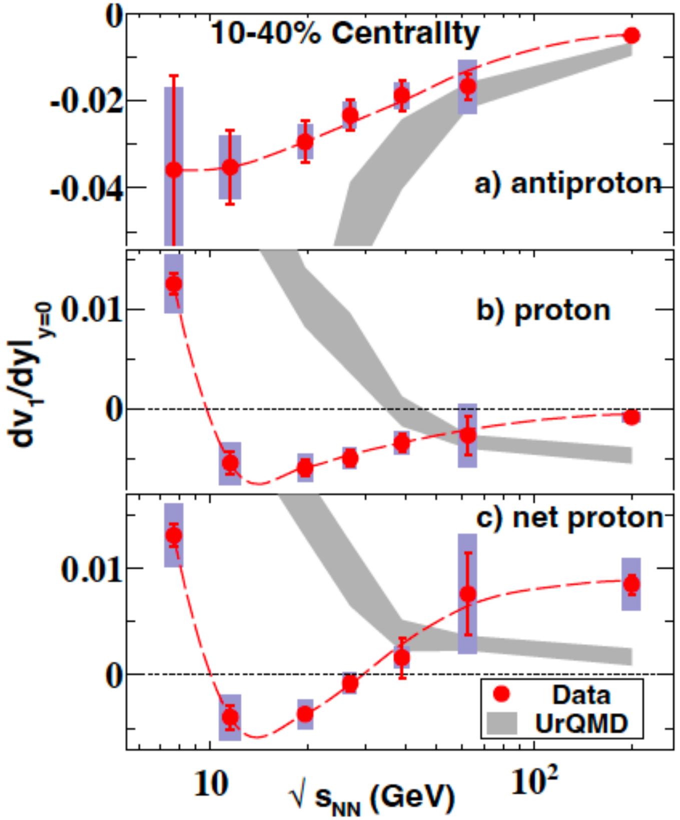

v_1 slope near midrapidity for antiprotons is negative

Proton slope changes sign

Net-proton slope changes sign twice

Vorticity of multi-strange hadrons

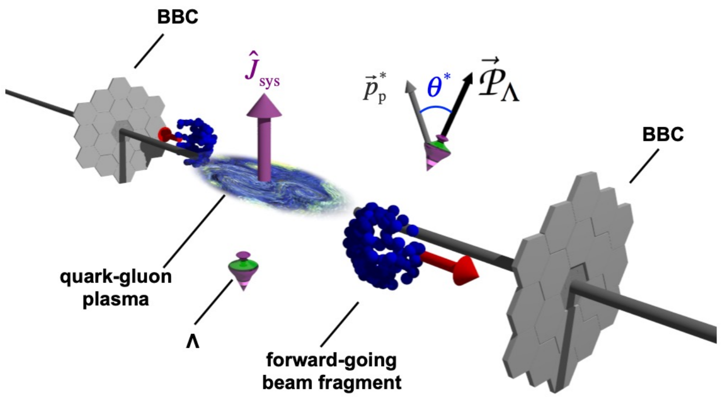

Global angular momentum transfer to hyperon polarization

Heavy ion collisions created the most vortical system ever observed.

Nature **548** (2017) 62

PRL126 (2021) 162301

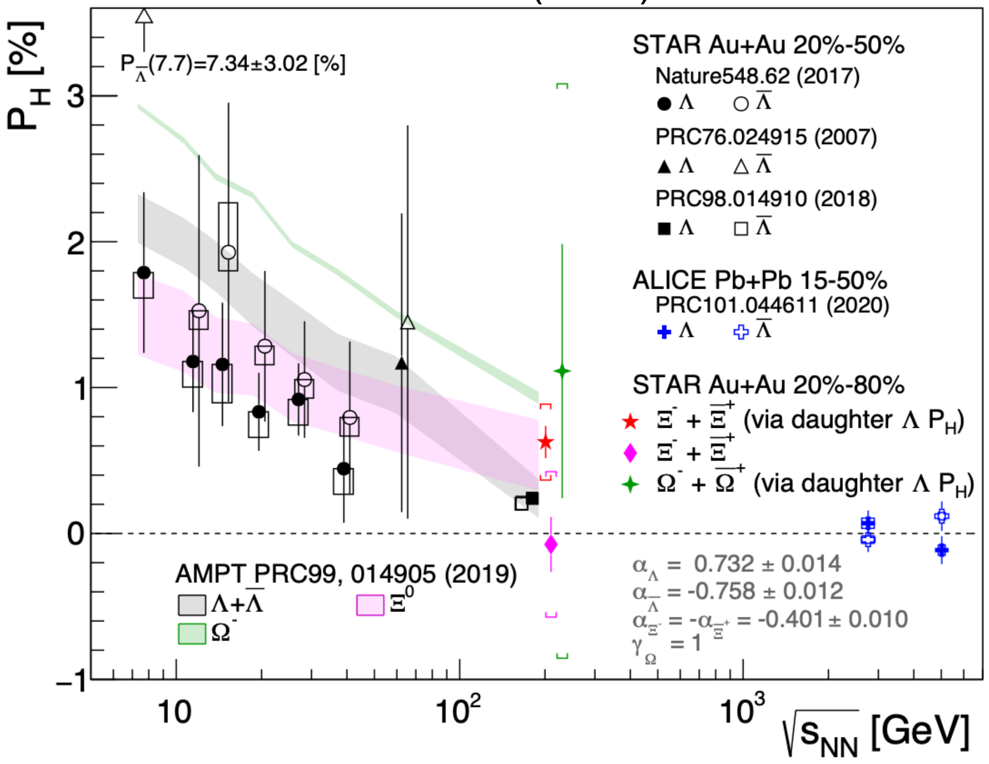

$\langle P_\Lambda \rangle$ (%) = 0.24 ± 0.03 (stat) ± 0.03 (syst)
$\langle P_\Xi \rangle$ (%) = 0.47 ± 0.10 (stat) ± 0.23 (syst)
$\langle P_\Omega \rangle$ (%) = 1.11 ± 0.87 (stat) ± 1.97 (syst)

First measurement of global polarization of Ξ and Ω

Results reinforce picture of system fluid vorticity

STAR beam energy scan phase II campaign

STAR Collaboration Decadal Plan
December 2010

1

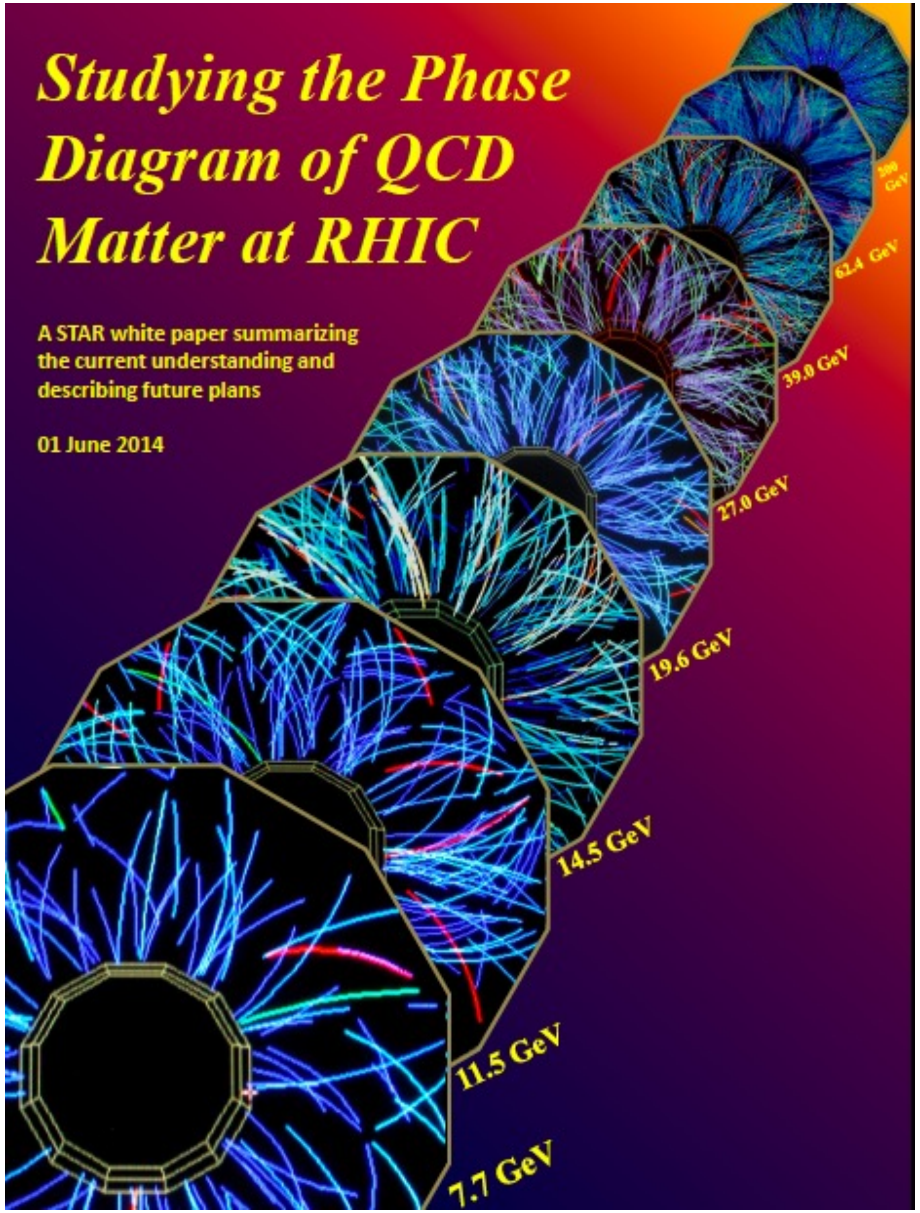

https://drupal.star.bnl.gov/STAR/starnotes/public/sn0598

STAR as a fixed-target experiment

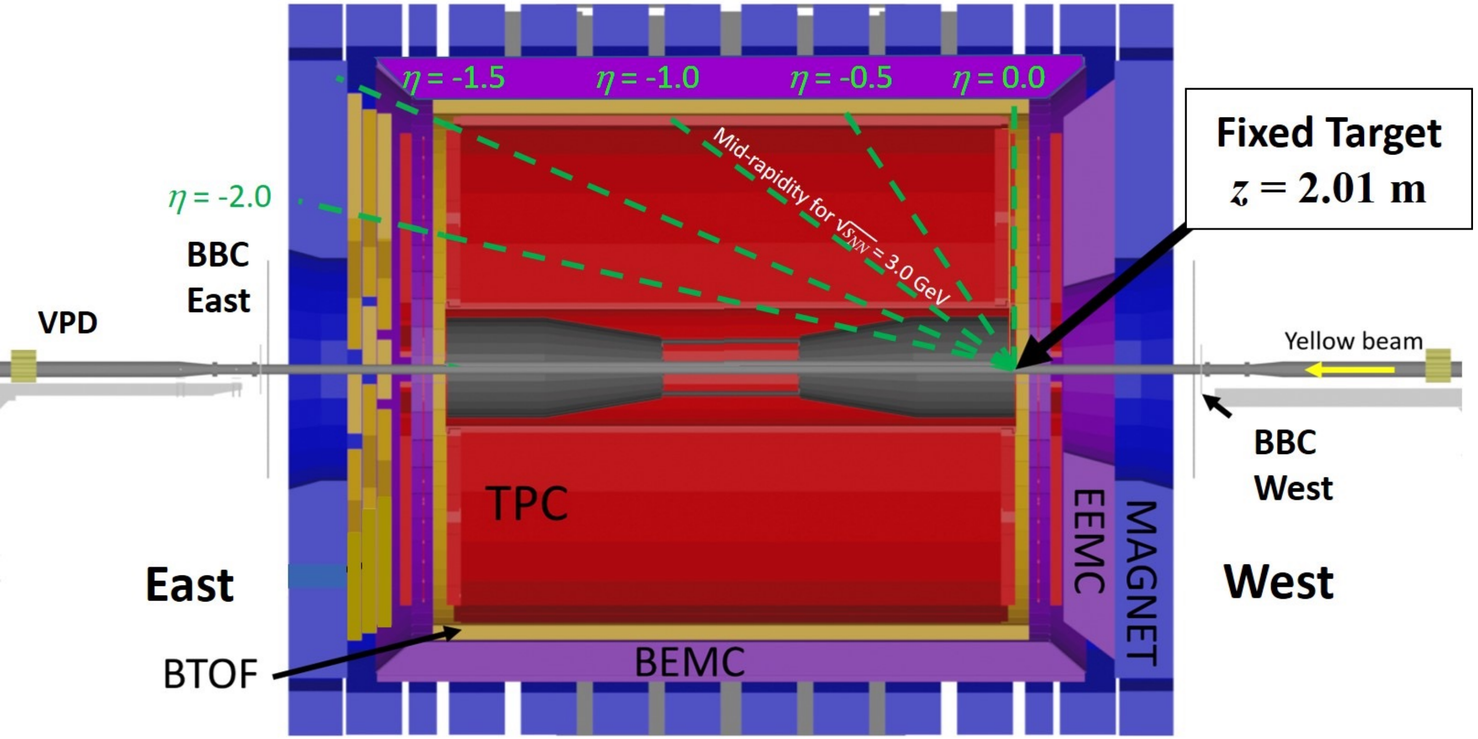

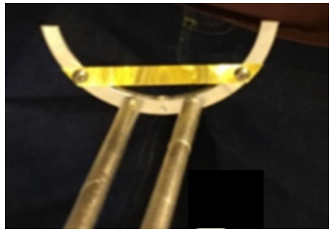

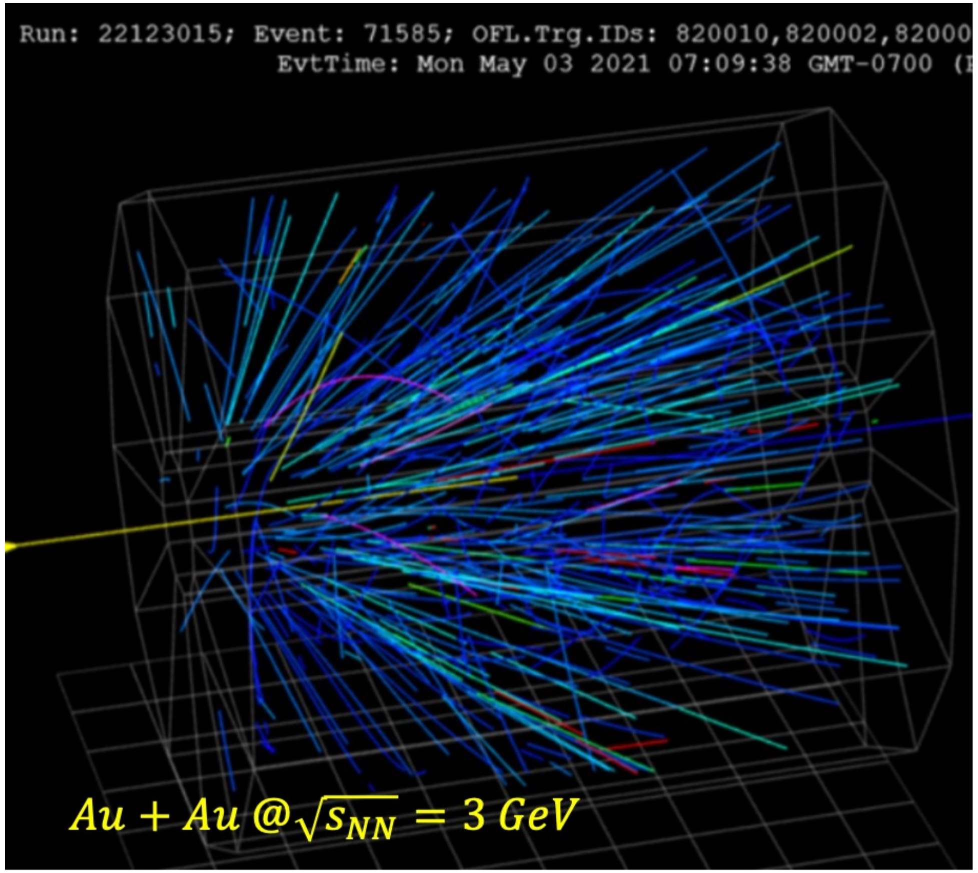

A gold target was installed inside the beam pipe in 2014

Net-proton higher moments at 3 GeV from FXT

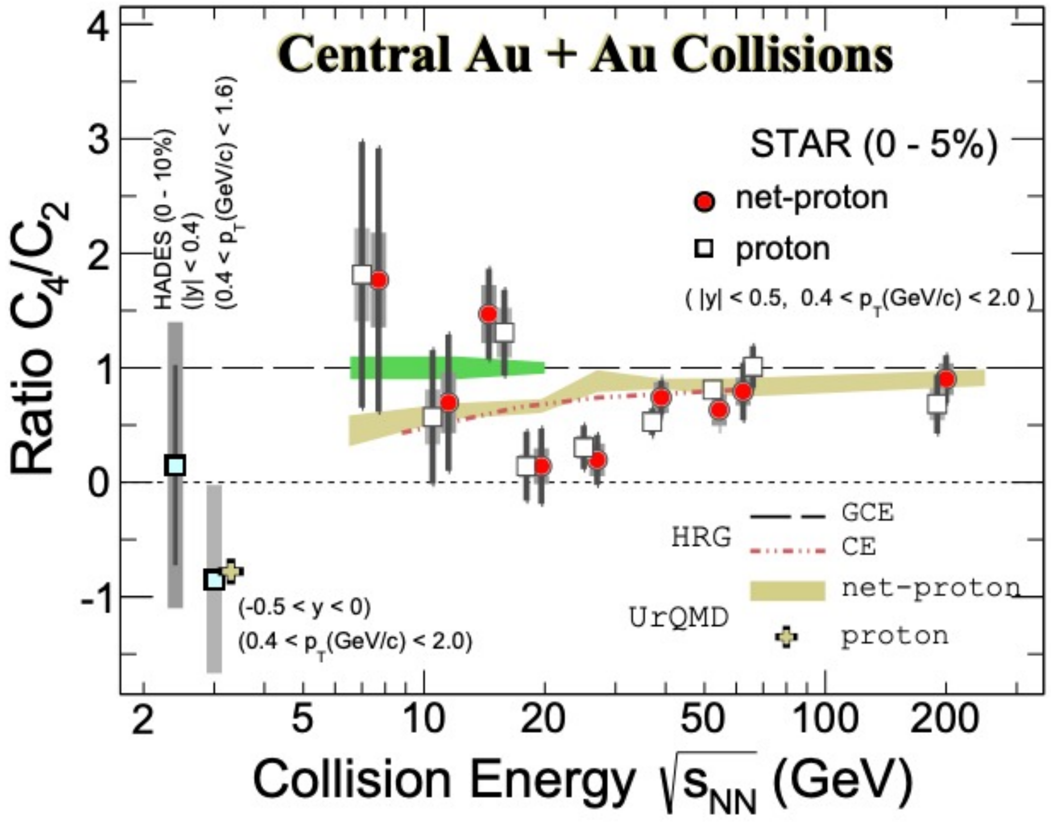

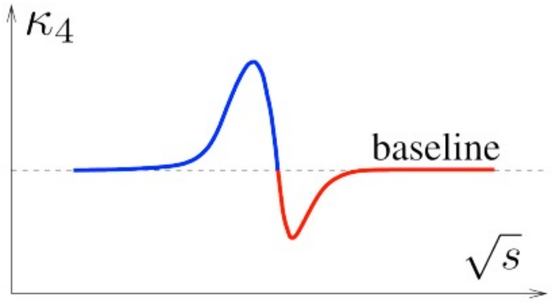

- Non-monotonic energy dependence in central Au+Au collisions (3.1σ)

- Strong suppression in proton C_4/C_2 at 3 GeV
  - *consistent with UrQMD hadronic transport model calculation*

BES-I: PRL 126 (2021) 092301
3 GeV data: PRL 128 (2022) 202303

BES-II data collected at RHIC will cover a broad and interesting range of μ_B for the critical point search

Higher order net-proton number fluctuations

PRL 130 (2023) 82301

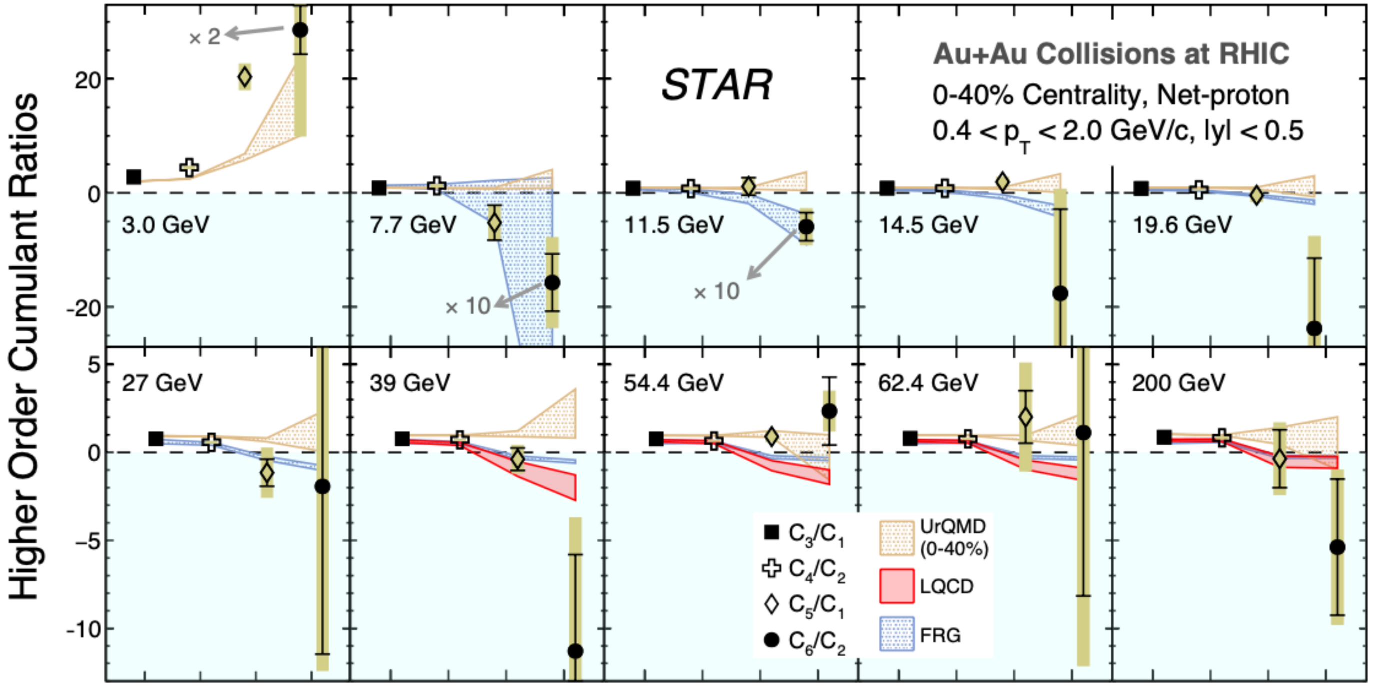

Calculations with a cross-over quark-hadron transition (LQCD and FRG) predict
a particular ordering of susceptibility ratios:

$$\chi_3^B/\chi_1^B > \chi_4^B/\chi_2^B > \chi_5^B/\chi_1^B > \chi_6^B/\chi_2^B$$

- At 7.7-200 GeV, net-proton cumulant ratios consistent with the ordering predicted by LQCD and FRG:
  $$C_3/C_1 > C_4/C_2 > C_5/C_1 > C_6/C_2$$
- The 3 GeV data show a reversing trend

The structure of QCD matter at high baryon density μ_B ~720 MeV starkly different from those at vanishing μ_B

Disappearance of partonic collectivity in 3 GeV Au+Au collisions

Phys. Lett. B **827** (2022) 137003

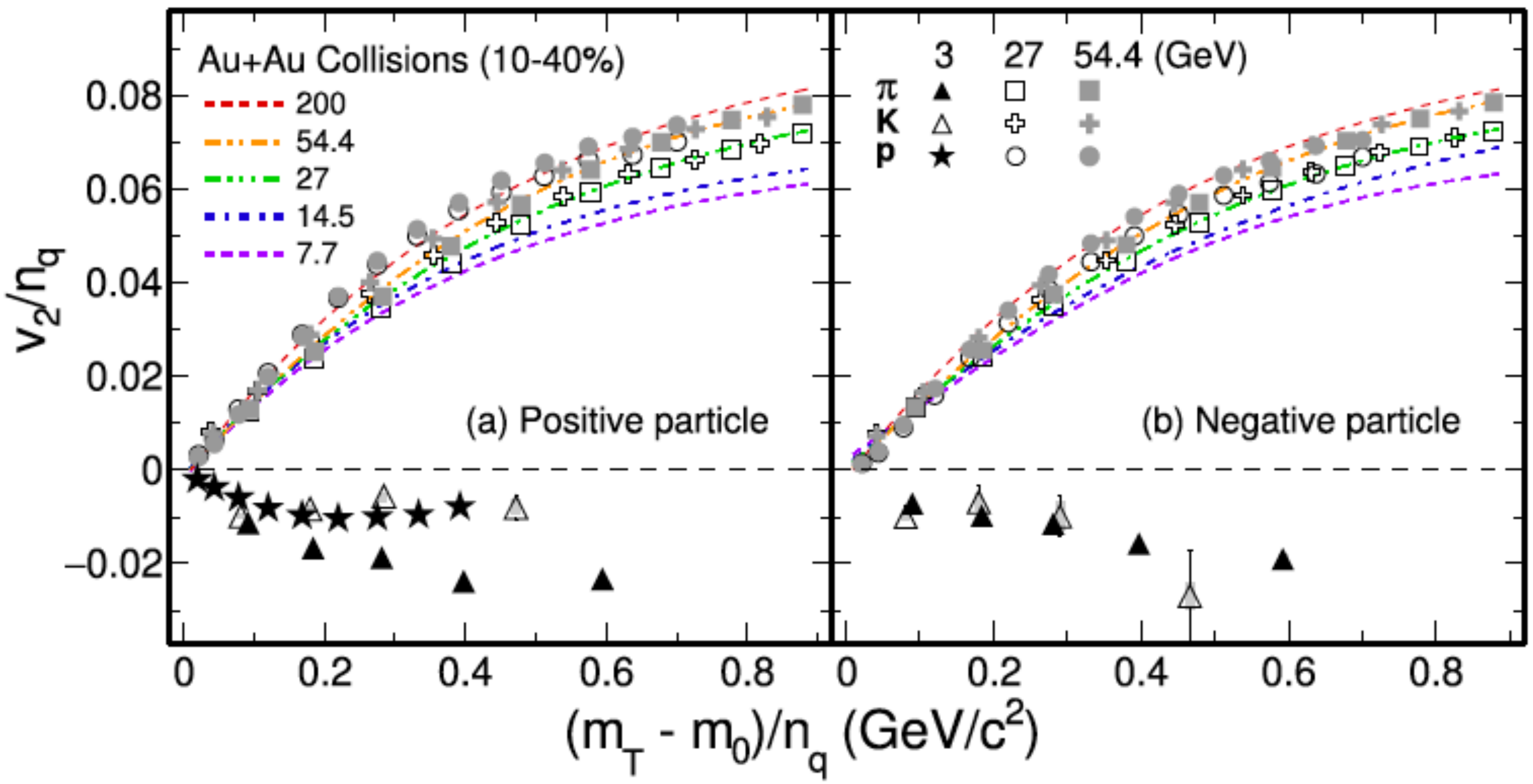

- Number of constituent quark (NCQ) scaling holds at 14.5 GeV and above
- No NCQ scaling and negative elliptic flow observed at 3 GeV

The results can be reproduced with a baryonic mean-field in transport model calculations.

Baryonic interactions dominate in 3 GeV Au+Au collisions

Directed flow of hypernuclei

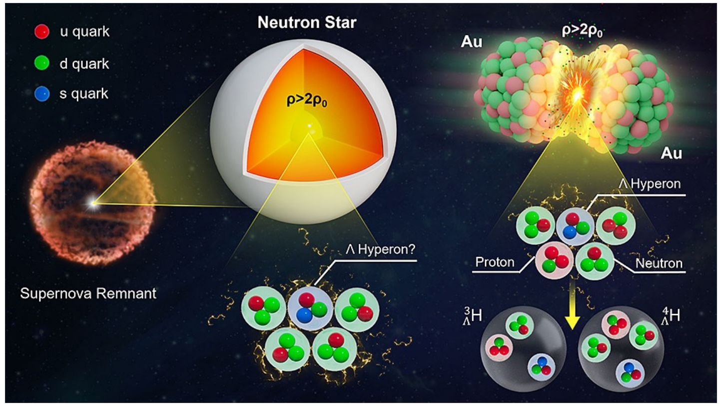

Picture credit:
BNL news article
https://www.bnl.gov/newsroom/news.php?a=121192

Hypernuclei Production

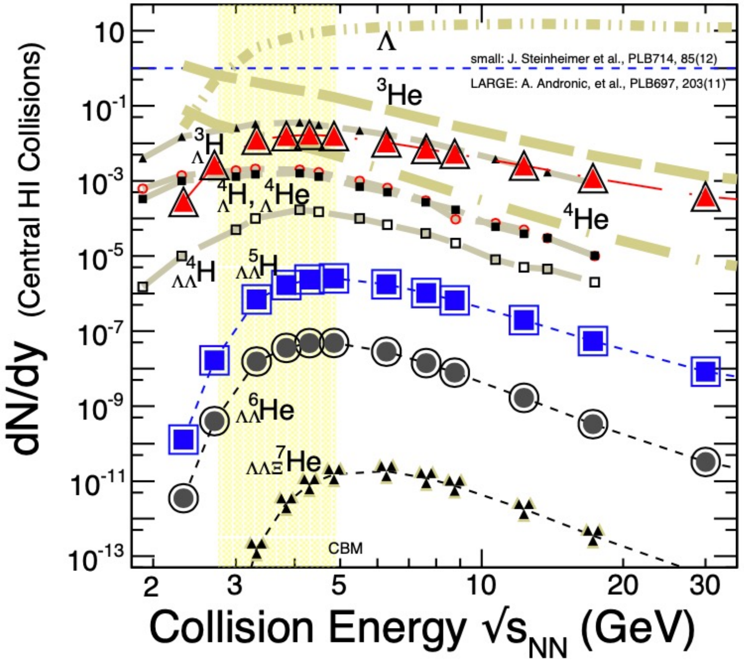

Constrain hyperon – nucleon and hyperon-hyperon interaction
Connection to neutron stars

PRL 130 (2023) 212301

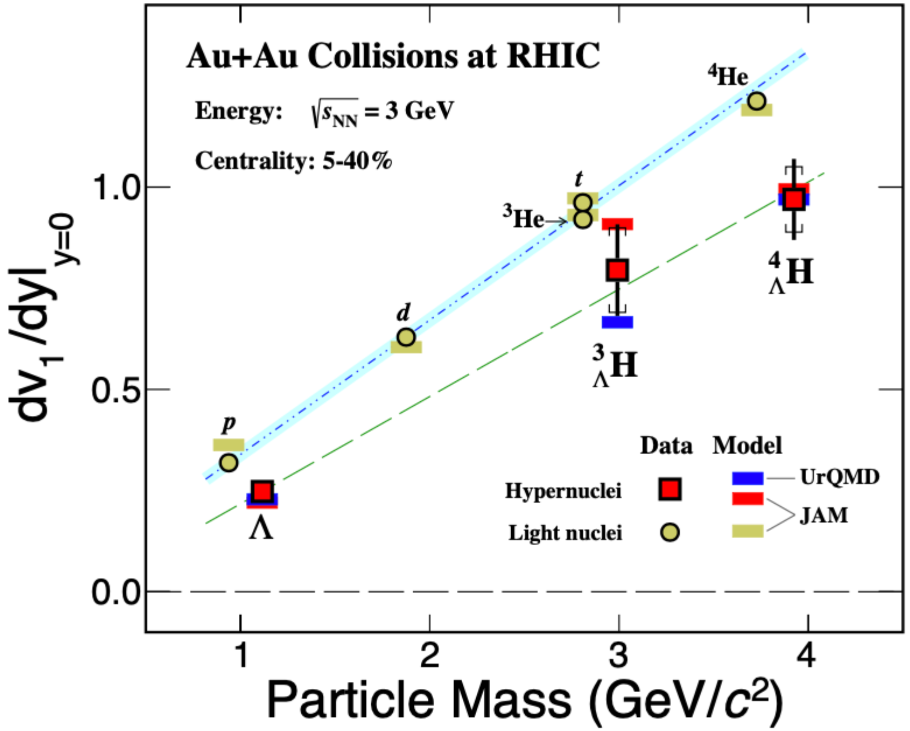

- First observation of significant hypernuclei directed flow in high energy nuclear collisions
- Midrapidity v_1 slopes follow baryon number scaling, implying that coalescence is the dominant production mechanism

Constrain hyperon-nucleon interactions at high baryon density

STAR BES-II upgrades

Major improvements for BES-II

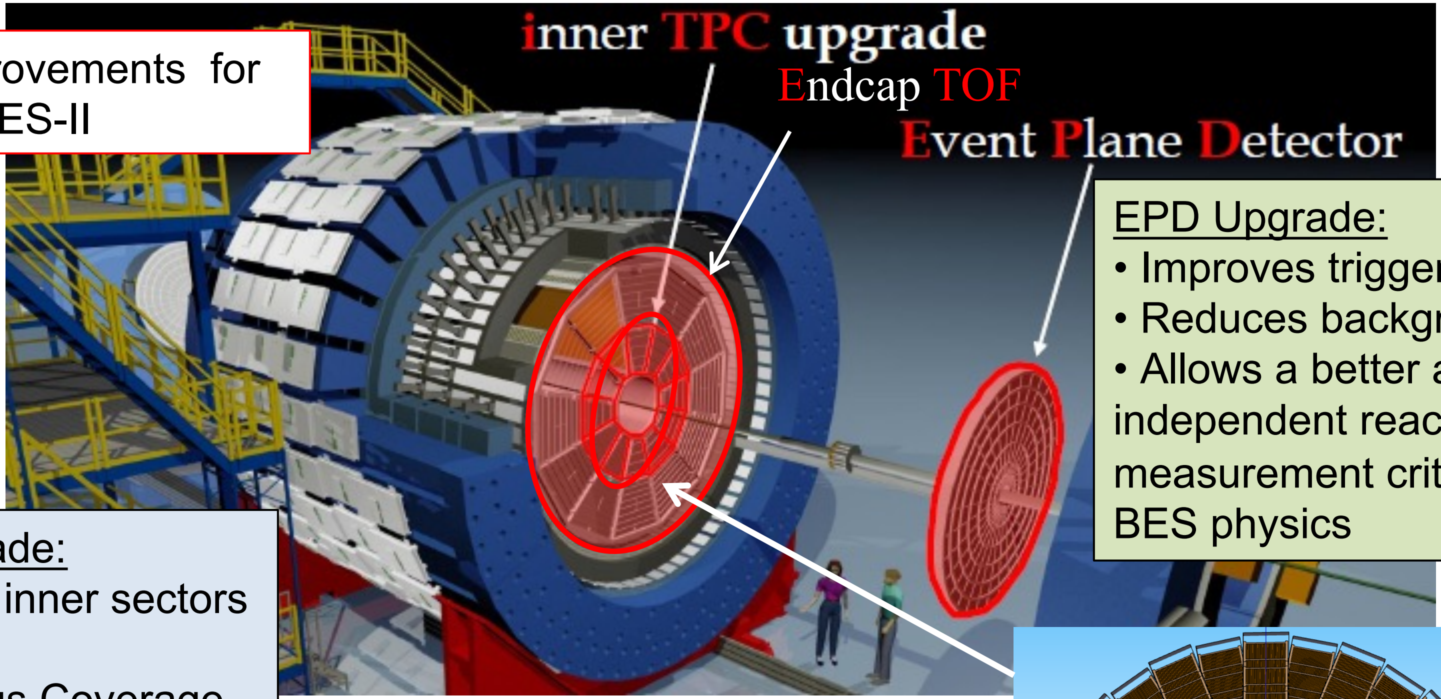

EPD Upgrade:
- Improves trigger
- Reduces background
- Allows a better and independent reaction plane measurement critical to BES physics

iTPC Upgrade:
- Replaced inner sectors of the TPC
- Continuous Coverage
- Improves dE/dx
- Extends η coverage from 1.0 to 1.5
- Lowers p_T cut from 125 MeV/c to 60 MeV/c

EndCap TOF Upgrade:
- Rapidity coverage is critical
- PID at η = 1 to 1.5
- Improves the fixed target program
- Provided by CBM-FAIR

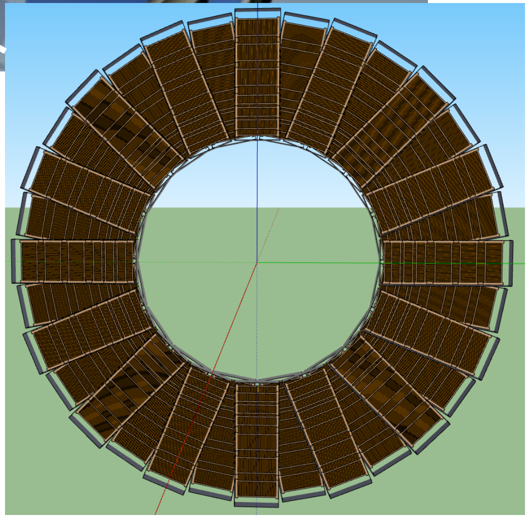

Detector performance

iTPC (2019+)

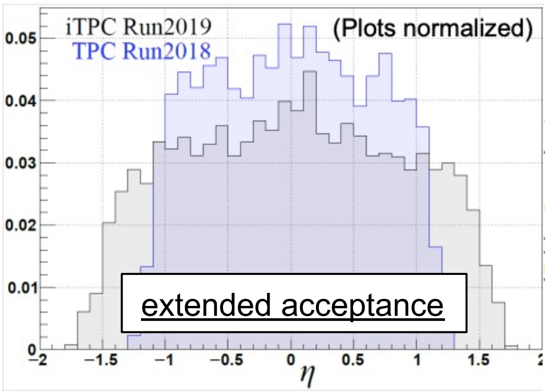

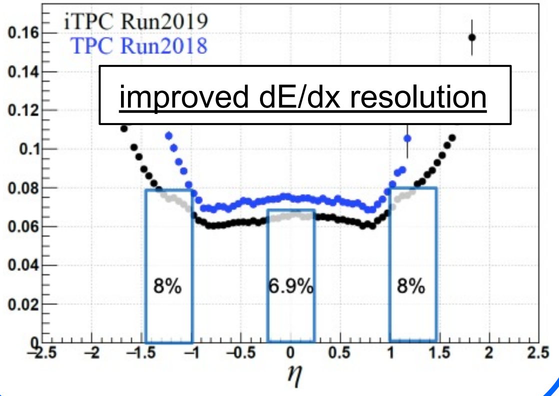

eTOF (2019+)

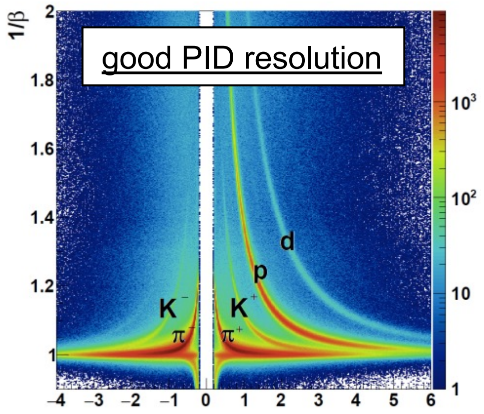

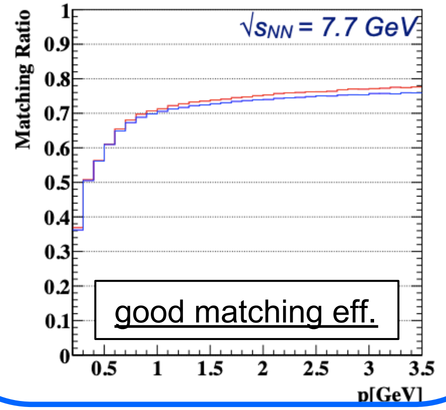

EPD (2018+)

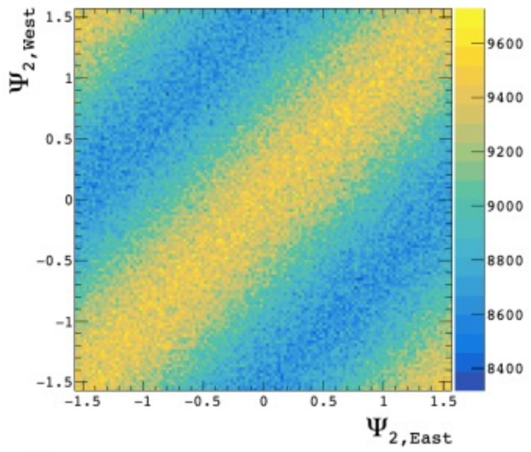

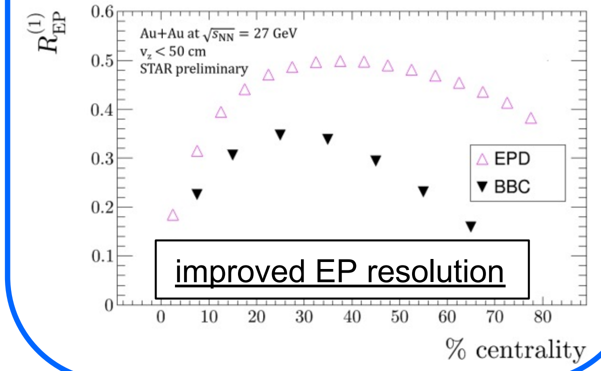

Beam energy scan phase II (BES-II) in 2019-2021

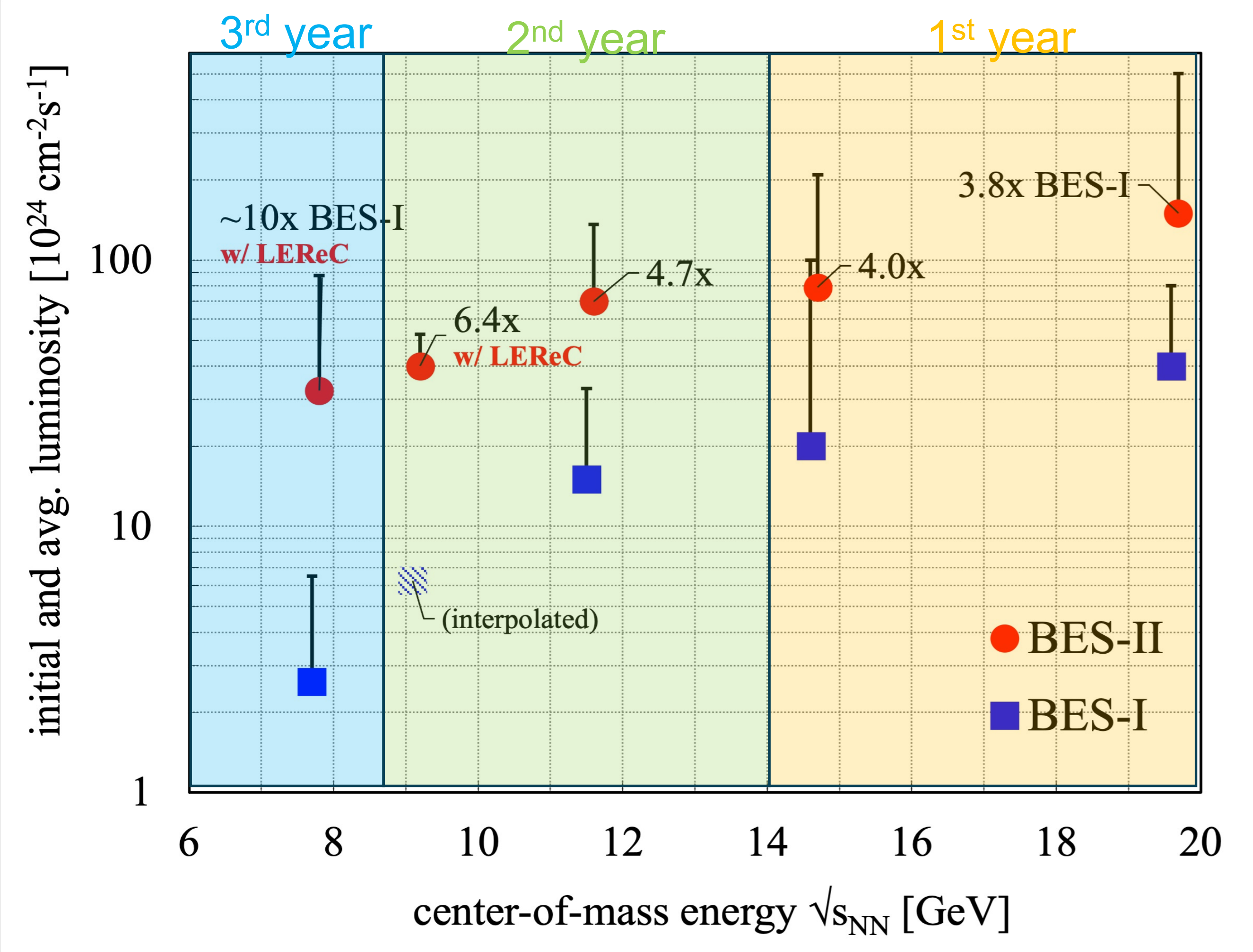

Goal was L_{avg} (BES-II) = 4x L_{avg} (BES-I)

In BES-II

3.8 x L_{avg} (BES-I)
4.0 x L_{avg} (BES-I)

4.7 x L_{avg} (BES-I)
6.4 x L_{avg} (BES-I)

~10 x L_{avg} (BES-I)

with LEReC at lowest beam energies

LEReC: low energy RHIC electron cooling

RHIC is unique to map the phase diagram of QCD:

Beam energy scan II: collision energies 7.7, 9.2, 11.5, 14.6, 17.3, 19.6 GeV and 12 fixed-target energies

In 2021, collected the last collider data set at 7.7 GeV, completed the BES-II program.

BES-II datasets

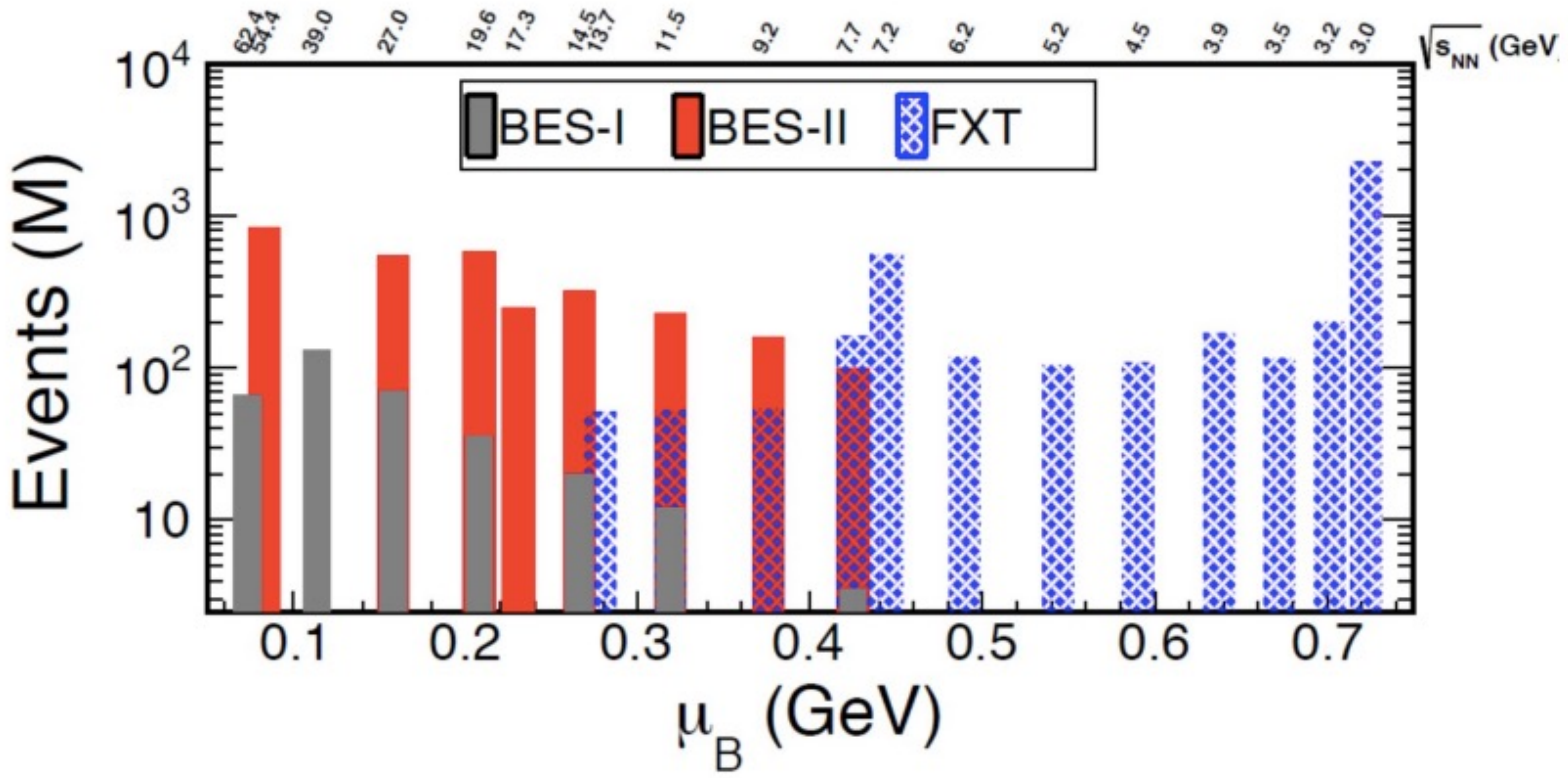

A broad μ_B coverage: $20 < \mu_B < 720$ MeV

BES-II data collected at RHIC will cover a broad and interesting range of μ_B for the critical point search

Net-proton higher moments from BES-II from 7.7 GeV to 27 GeV

156 < μ_B < 420 MeV

See Yige Huang's talk in the afternoon

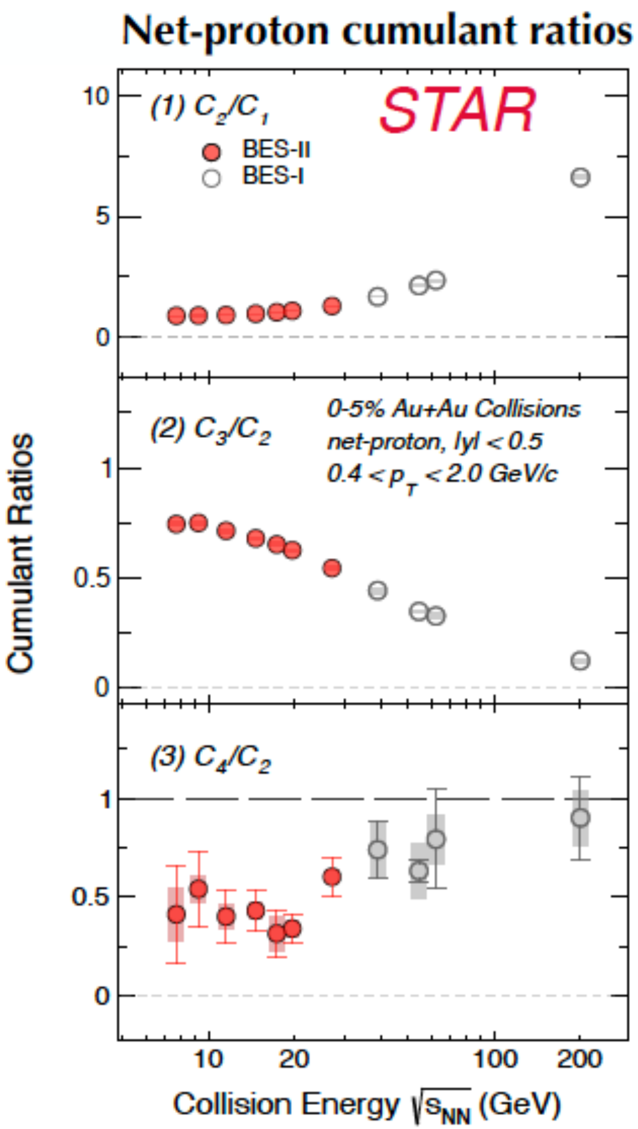

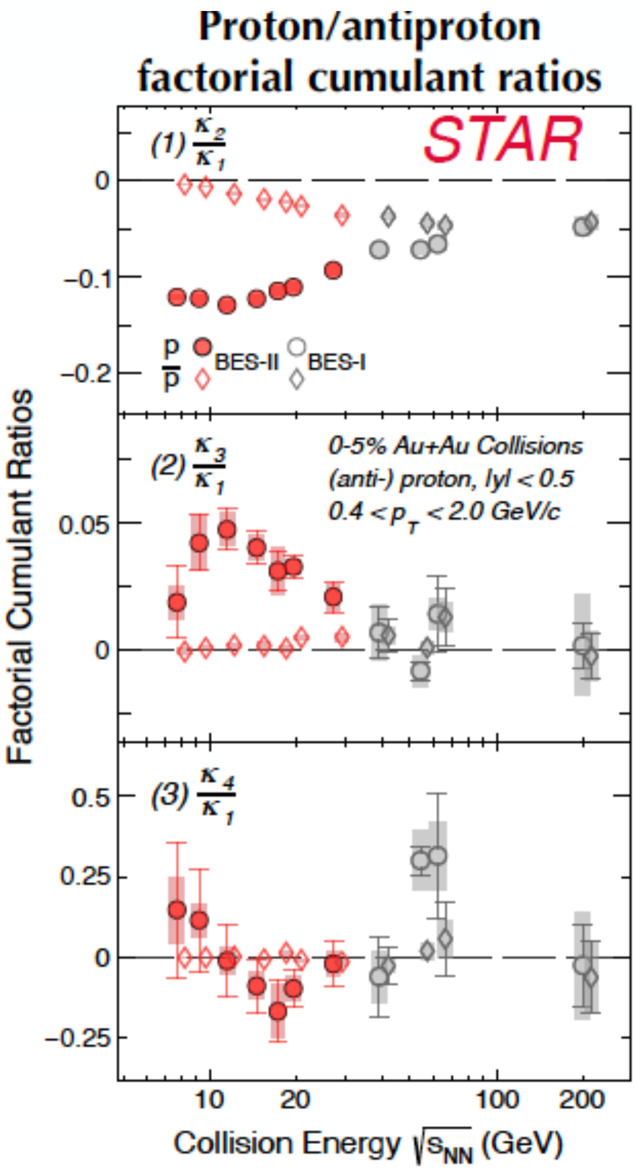

Reduction factor in uncertainties on 0-5% C_4/C_2 : BES-II vs BES-I

7.7 GeV		19.6 GeV	
stat. error	sys. error	stat. error	sys. error
4.7	3.2	4.5	4

Very interesting trends observed as a function of collision energy

The phases of QCD matter

The 2023 NSAC Long Range Plan for Nuclear Science

Lattice QCD: crossover chiral transition at $\mathbf{\mu_B < 2\,T}$

At top RHIC and LHC energies, measurements consistent with a smooth crossover chiral transition

RHIC Beam Energy Scan Phase I (BES-I) measurements imply the QCD critical point, if exists, should be accessible in the center of mass energy region 3-20 GeV

BES-II data taking (energy range 3 - 19.6 GeV) completed in 2021, physics analyses under active pursuit need to be completed

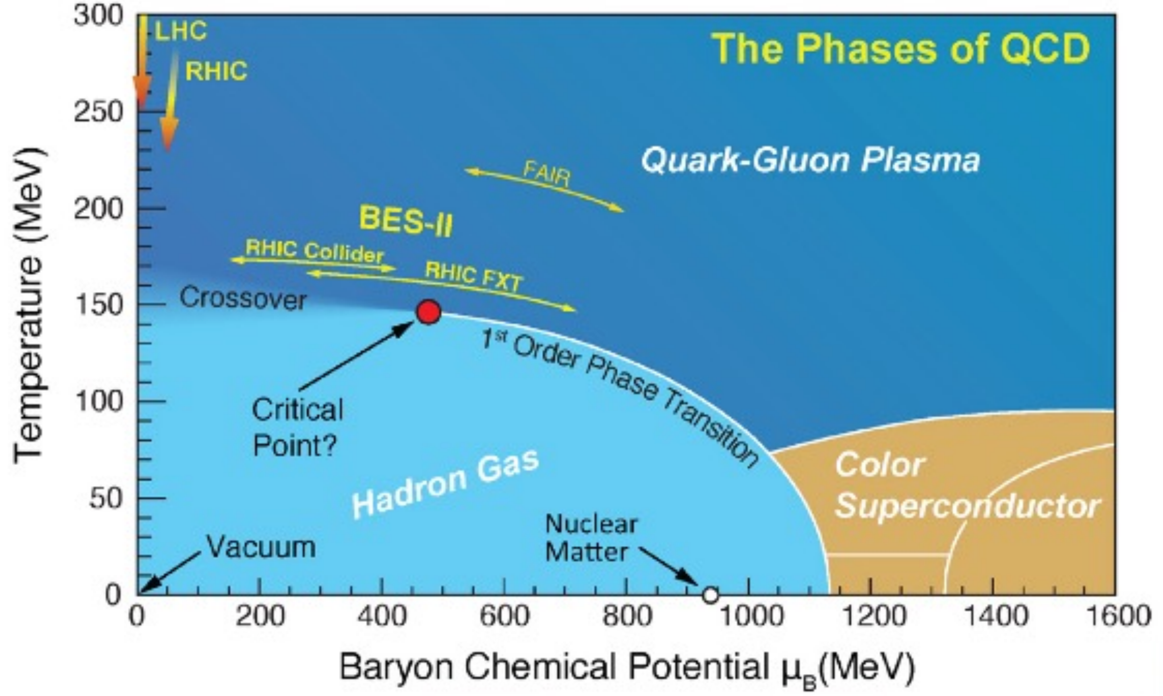

Future experiments, such as CBM at FAIR in Germany will provide additional high statistics and high-resolution data for low-energy collisions and high μ_B

The future

NA60⁺ (2029)

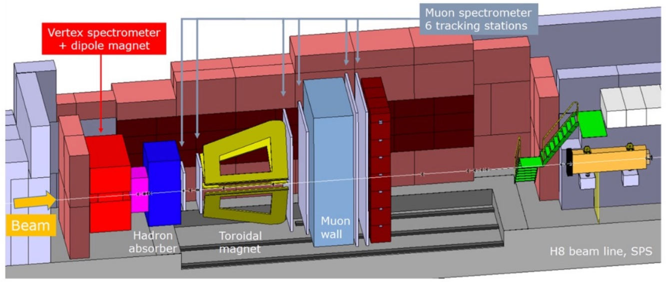

NA61 (2008 - 2027)

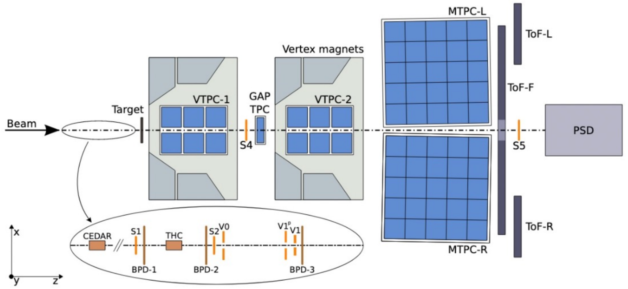

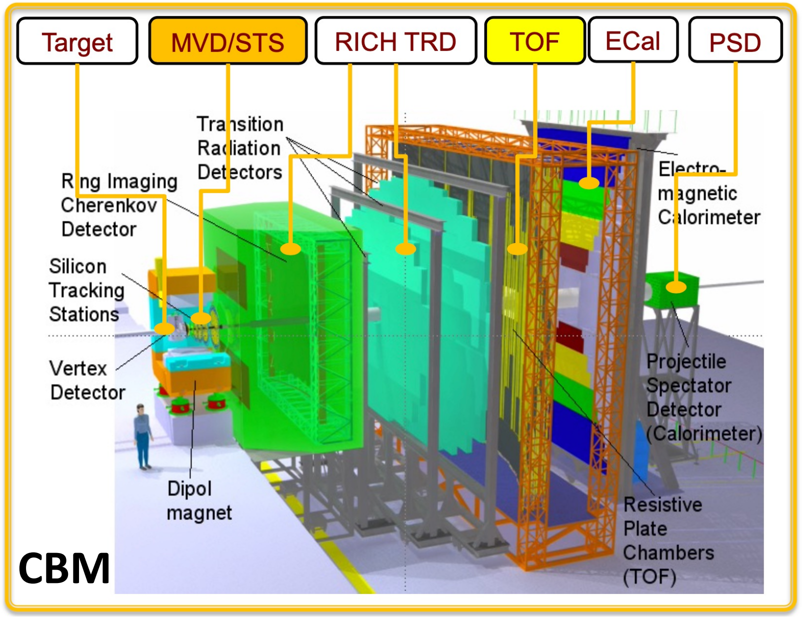

Physics opportunities in the exploration of the QCD phase diagram at high baryon density after the completion of the RHIC BES-II program: NA60+, NA61, CBM, NICA …

Probe the physics of dense baryon-rich matter and constrain the nuclear equation of state in a regime relevant to binary neutron star mergers and supernovae.

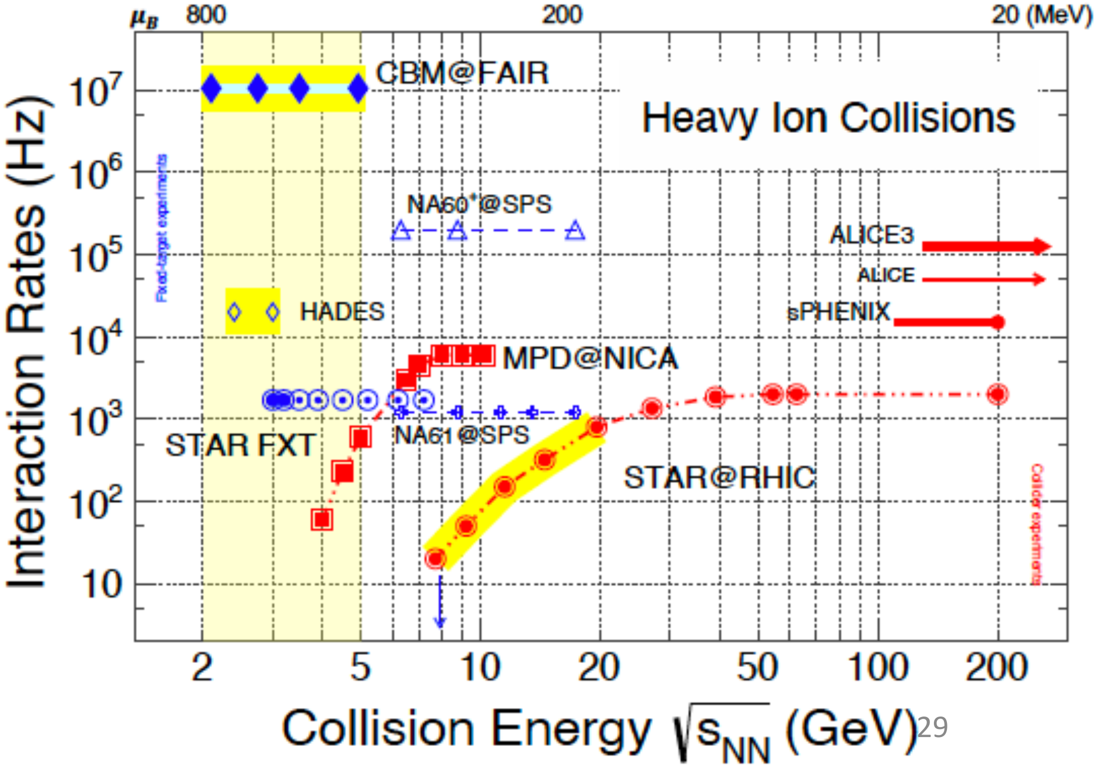

Backup

Identified particle charge-dependent v_1

STAR, arXiv: 2304.03430

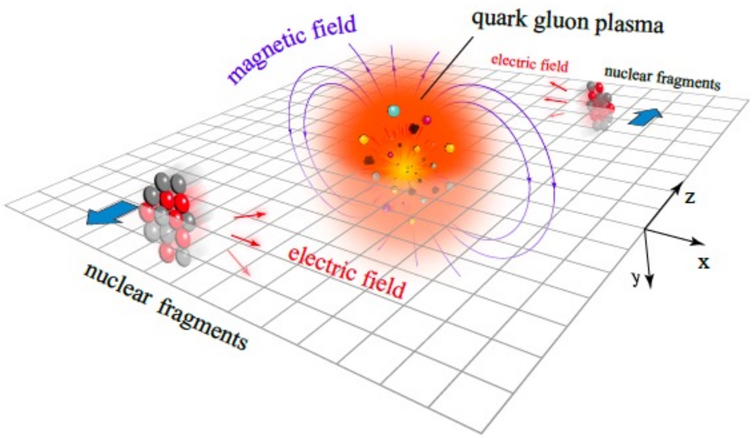

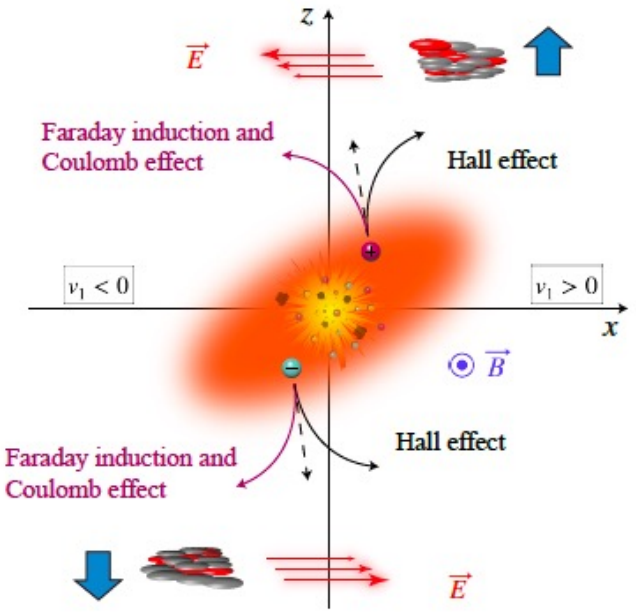

Transported-quark effect:
positive charge-dependent v1 slope

Faraday + Coulomb:
negative charge-dependent v1 slope

Hall effect:
positive charge-dependent v1 slope

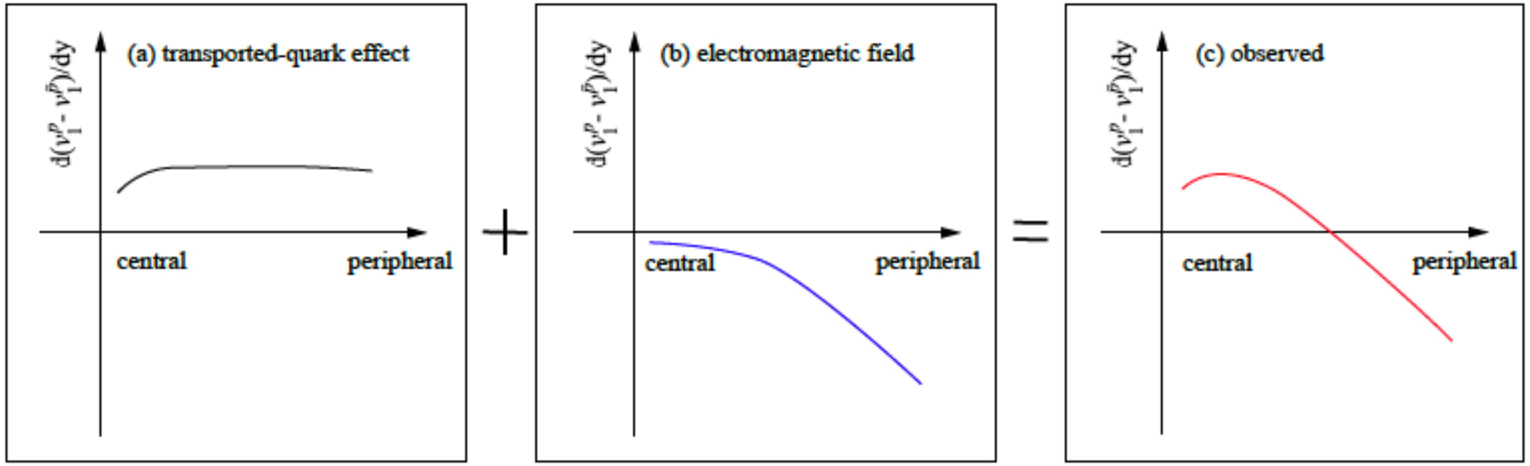

Identified particle charge-dependent v_1

STAR, arXiv: 2304.03430, accepted by PRX

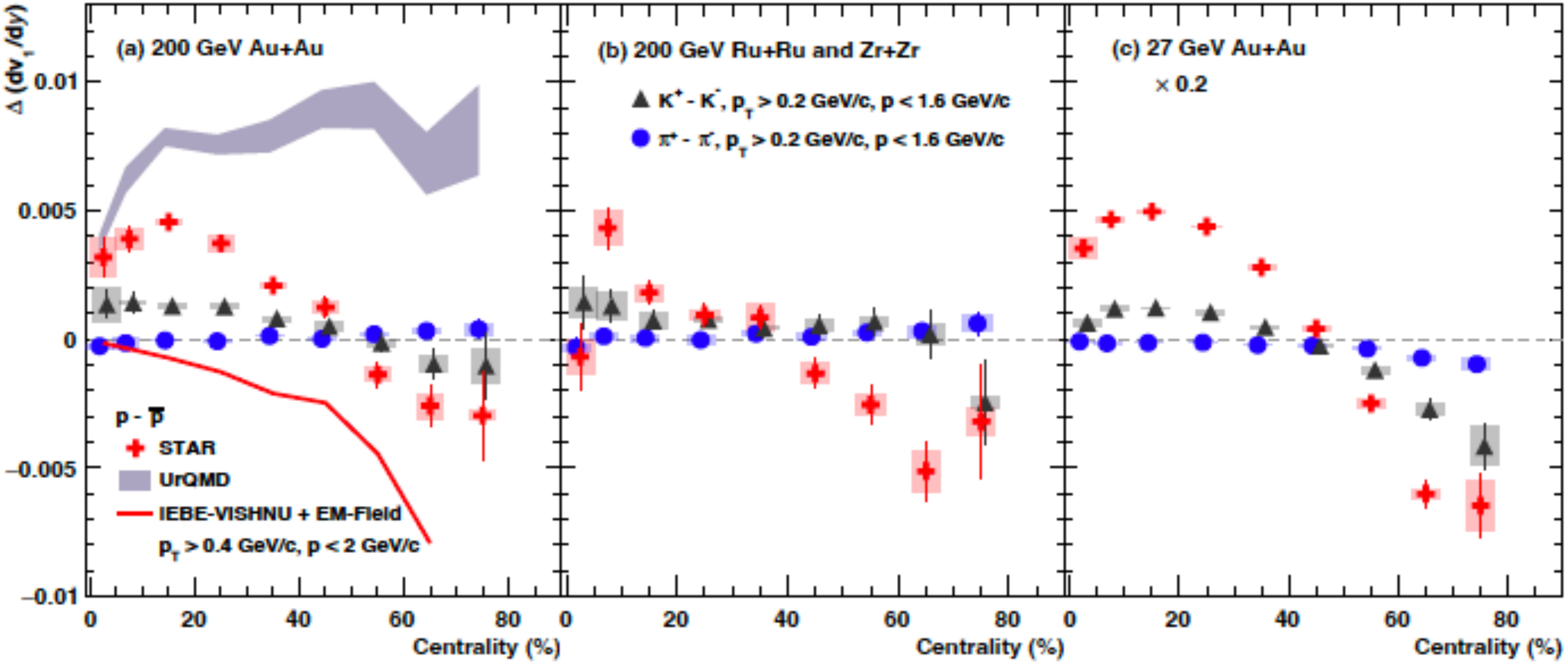

Results in central collisions can be explained by transported quark effect

Results in peripheral collisions consistent with the Faraday induction and Coulomb effect

Beam energy scan phase II (BES-II) in 2019-2021

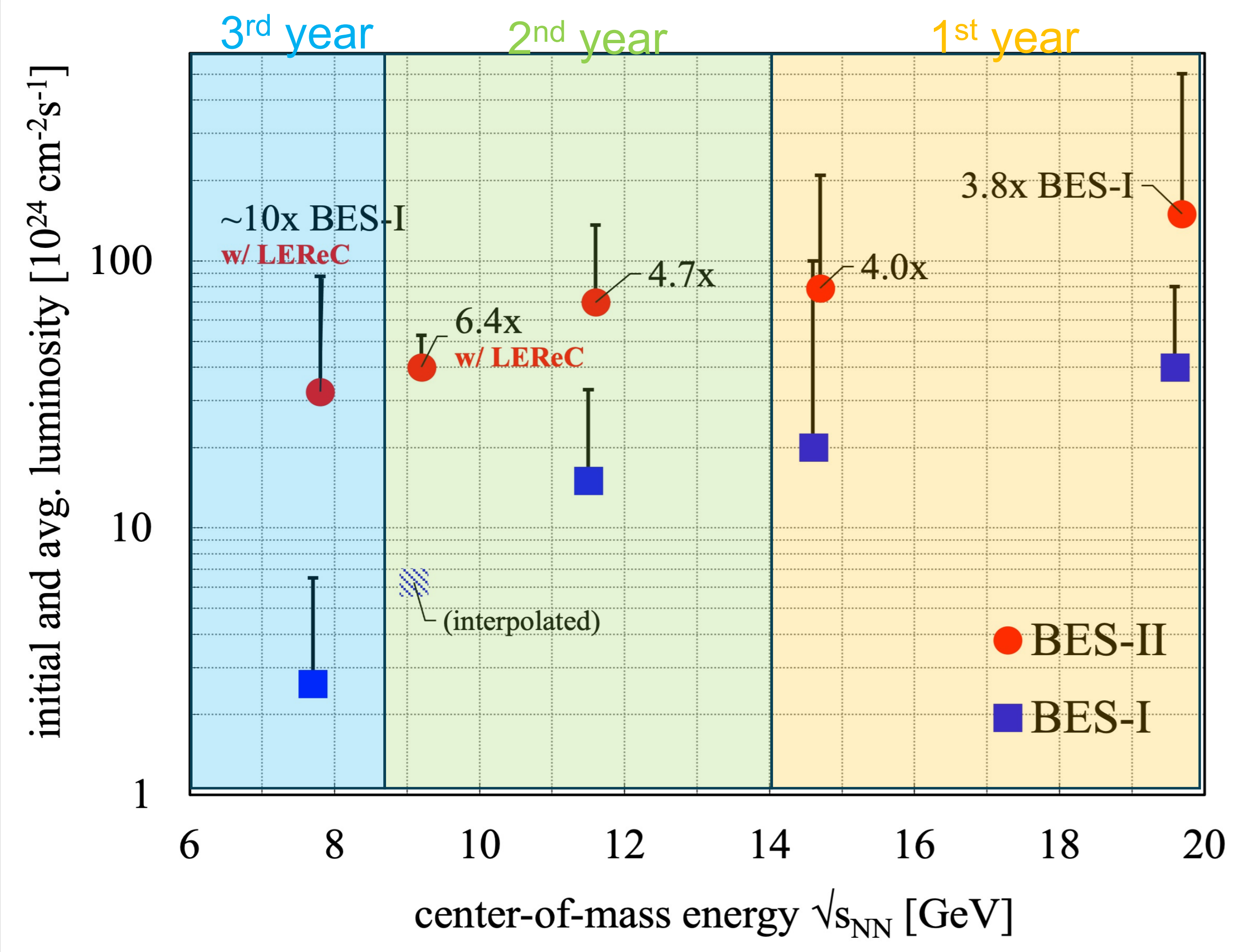

Goal was L_{avg} (BES-II) = 4x L_{avg} (BES-I)

In BES-II

3.8 x L_{avg} (BES-I)
4.0 x L_{avg} (BES-I)

4.7 x L_{avg} (BES-I)
6.4 x L_{avg} (BES-I) ⬅

~10 x L_{avg} (BES-I) ⬅

with LEReC at lowest beam energies

LEReC: low energy RHIC electron cooling

RHIC is unique to map the phase diagram of QCD:

Beam energy scan II: collision energies 7.7, 9.2, 11.5, 14.6, 17.3, 19.6 GeV and 12 fixed-target energies

In 2021, collected the last collider data set at 7.7 GeV, completed the BES-II program.

Physics at high baryon density frontier

US-CBM white paper

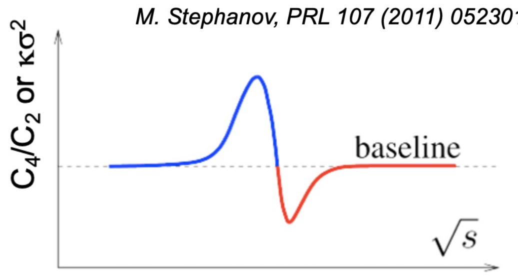

Critical Fluctuations

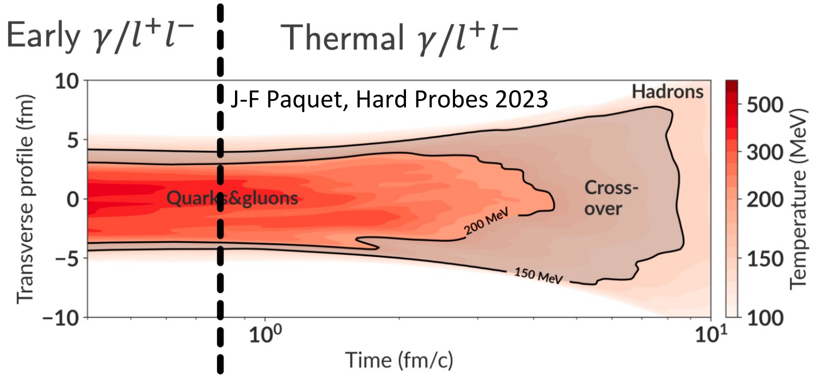

Thermal Radiation

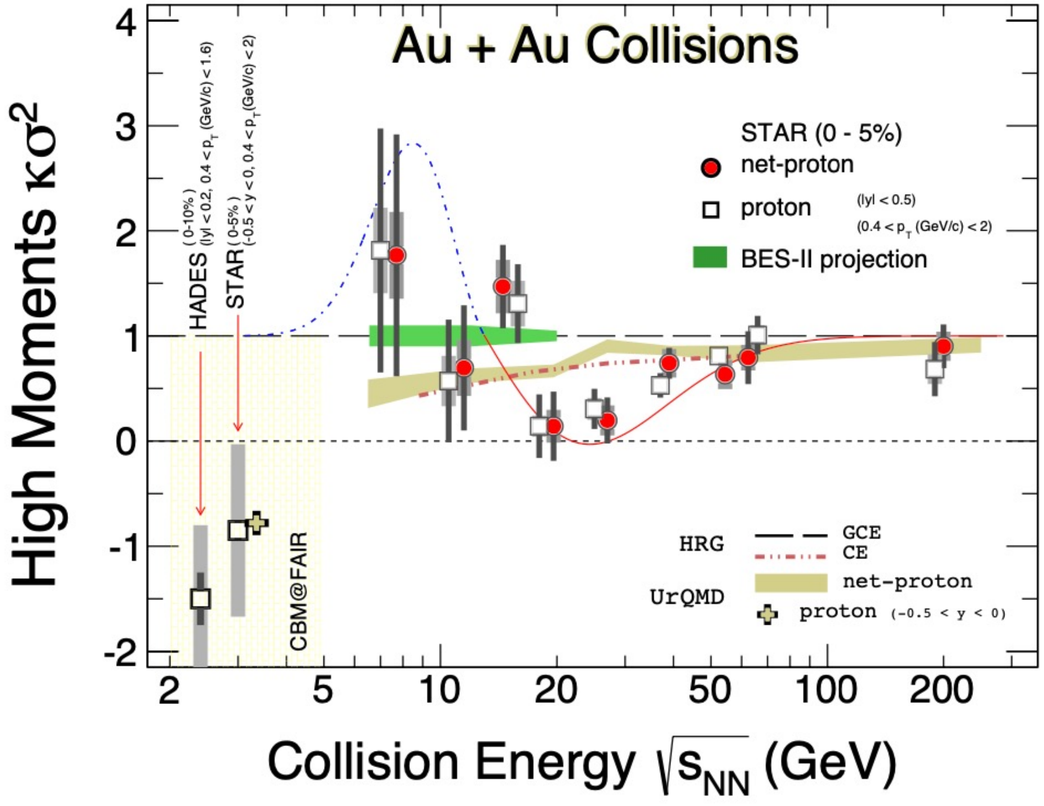

Search for the QCD critical point

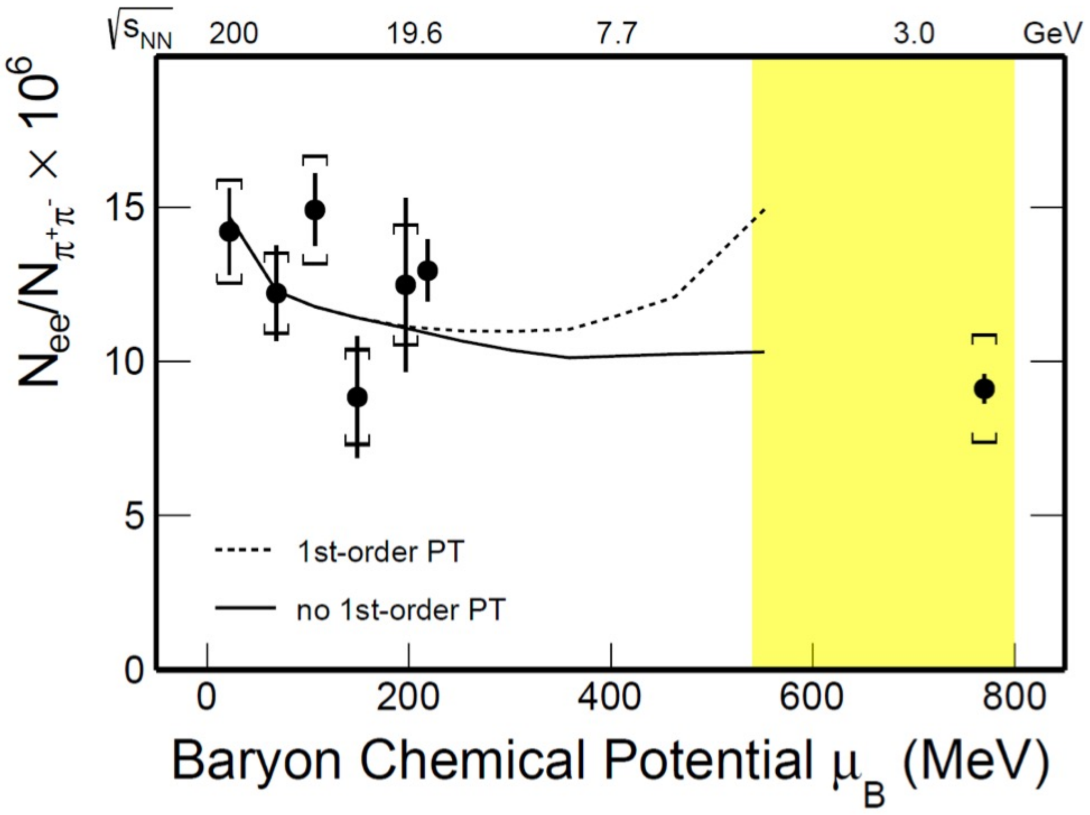

Probe first order phase transition

Physics at high baryon density frontier

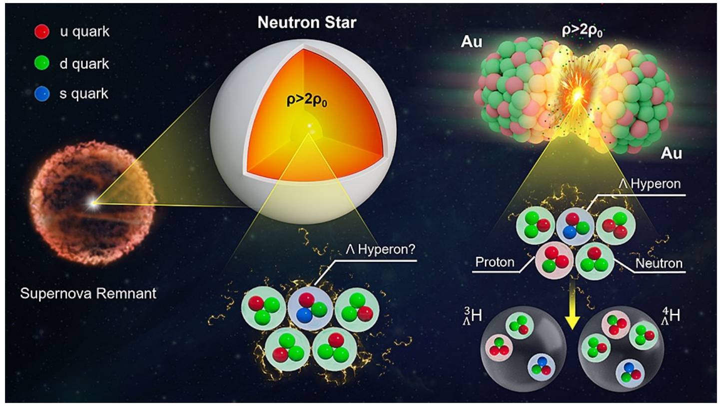

Picture credit:
BNL news article
https://www.bnl.gov/newsroom/news.php?a=121192

US-CBM white paper

Hypernuclei Production

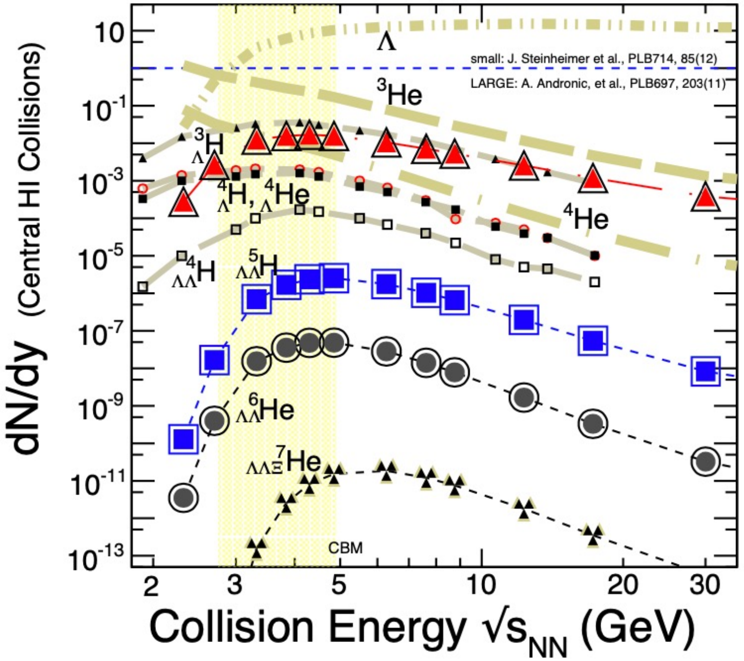

Constrain hyperon – nucleon and hyperon-hyperon interaction
Connection to neutron stars

Nature 548 (2017) 62

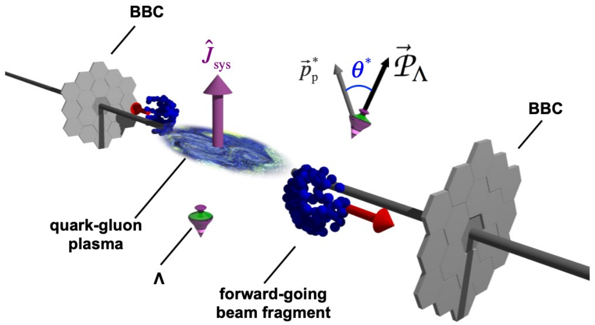

Polarization/Spin Alignment

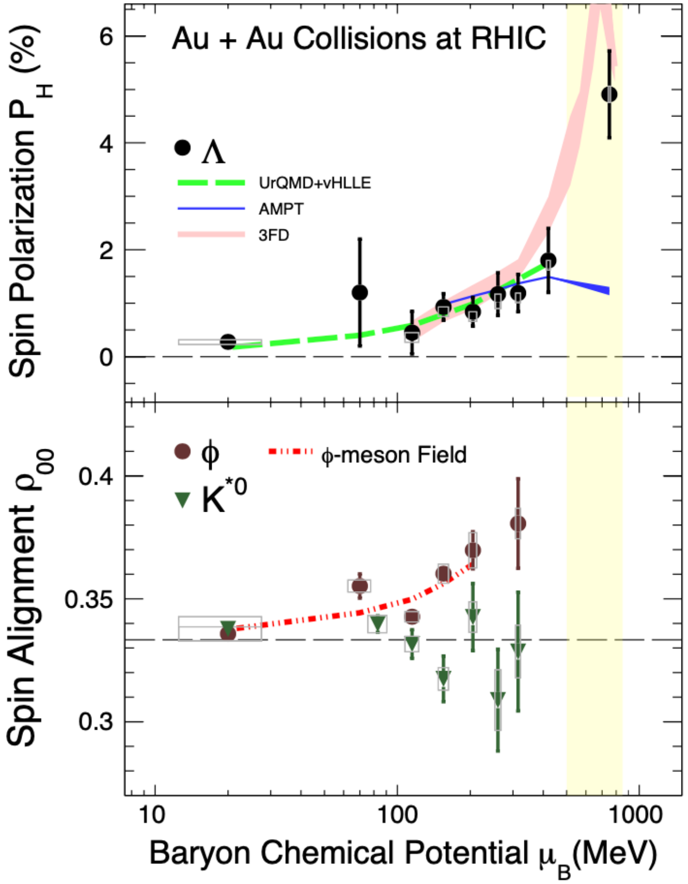

Probe vorticity field